Closed-loop microstimulations of the orbitofrontal cortex during real-life gaze interaction enhance dynamic social attention

Neuron

Article

Closed-loop microstimulations of the orbitofrontal cortex during real-life gaze interaction enhance dynamic social attention

Graphical abstract

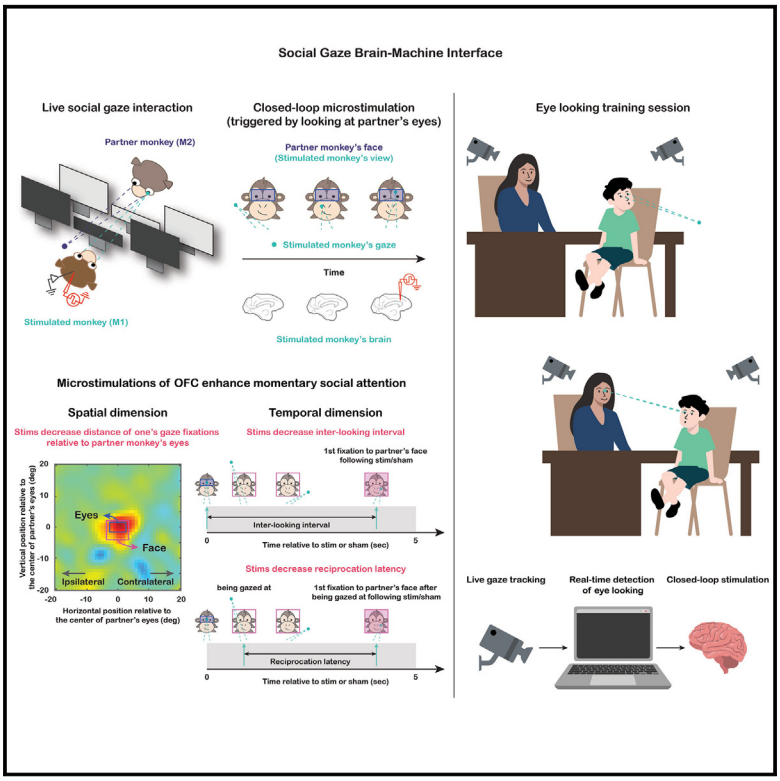

Highlights

- Closed-loop microstimulation was applied contingently upon looking at the other's eyes
- OFC microstimulations enhanced momentary spatial and temporal social attention
- dmPFC microstimulations affected longer-term inter-individual gaze dynamics
- Primate prefrontal cortex has causal nodes for controlling dynamic social attention

Authors

Siqi Fan, Olga Dal Monte, Amrita R. Nair, Nicholas A. Fagan, Steve W.C. Chang

Correspondence

steve.chang@yale.edu

In brief

Fan and Dal Monte et al. apply closed-loop microstimulations in prefrontal areas when monkeys interact with gaze. Stimulations of the orbitofrontal cortex enhance momentary spatial and temporal social attention, whereas stimulations of the dorsomedial prefrontal cortex modulate inter-individual gaze dynamics. These regions causally control social attention, with potential for therapeutic brain interface.

Fan et al., 2024, Neuron *112*, 2631–2644
August 7, 2024
https://doi.org/10.1016/j.neuron.2024.05.004

CellPress

Neuron

CellPress

Article

Closed-loop microstimulations of the orbitofrontal cortex during real-life gaze interaction enhance dynamic social attention

Siqi Fan,[1,2,7] Olga Dal Monte,[1,3,7] Amrita R. Nair,[1] Nicholas A. Fagan,[1] and Steve W.C. Chang[1,4,5,6,8,*]
[1]Department of Psychology, Yale University, New Haven, CT 06520, USA
[2]The Laboratory of Neural Systems, The Rockefeller University, New York, NY 10065, USA
[3]Department of Psychology, University of Turin, 10124 Torino, Italy
[4]Department of Neuroscience, Yale University School of Medicine, New Haven, CT 06510, USA
[5]Kavli Institute for Neuroscience, Yale University School of Medicine, New Haven, CT 06510, USA
[6]Wu Tsai Institute, Yale University, New Haven, CT 06510, USA
[7]These authors contributed equally
[8]Lead contact
*Correspondence: steve.chang@yale.edu
https://doi.org/10.1016/j.neuron.2024.05.004

SUMMARY

Neurons from multiple prefrontal areas encode several key variables of social gaze interaction. To explore the causal roles of the primate prefrontal cortex in real-life gaze interaction, we applied weak closed-loop microstimulations that were precisely triggered by specific social gaze events. Microstimulations of the orbitofrontal cortex, but not the dorsomedial prefrontal cortex or the anterior cingulate cortex, enhanced momentary dynamic social attention in the spatial dimension by decreasing the distance of fixations relative to a partner's eyes and in the temporal dimension by reducing the inter-looking interval and the latency to reciprocate the other's directed gaze. By contrast, on a longer timescale, microstimulations of the dorsomedial prefrontal cortex modulated inter-individual gaze dynamics relative to one's own gaze positions. These findings demonstrate that multiple regions in the primate prefrontal cortex may serve as functionally accessible nodes in controlling different aspects of dynamic social attention and suggest their potential for a therapeutic brain interface.

INTRODUCTION

The prefrontal cortex evolved to process a wide range of information to adaptively guide behaviors in complex environments.[1] For social animals, it has been hypothesized that the prefrontal cortex, and other brain regions, prioritize social information to successfully navigate volatile social environments involving multiple conspecifics in group settings.[2–5] In many primate species, social gaze plays a pivotal role in conveying essential social information,[6] and several prefrontal brain regions are known to exhibit selective neural activity for social gaze interaction.[7,8] Although multiple subregions in the primate temporal and posterior parietal cortices, including the gaze-following patch, have been widely implicated in the perceptual aspects of social gaze,[9–13] the prefrontal subregions are theorized to play critical functions in integrating social, affective, and motivational information to enable appropriate social gaze processing.[14,15]

The neural systems involved in social gaze interaction must distinguish social from non-social gaze events, and also mark significant interactive events such as mutual eye contact, to regulate social behaviors. This is likely facilitated by the continuous monitoring of one's own gaze and the other's gaze over time. Recent research in pairs of rhesus macaques has demonstrated that a large proportion of individual neurons in the prefrontal cortex, including the orbitofrontal cortex (OFC), the dorsomedial prefrontal cortex (dmPFC), and the gyrus of anterior cingulate cortex (ACCg), exhibit robust neural representations for gaze fixations directed toward the eyes and the face of a conspecific partner and for context-specific mutual eye contact events.[8] Importantly, a substantial proportion of cells in these areas were found to parametrically track the Euclidian distance of the monkey's own gaze fixations in space relative to a partner monkey's eyes and the distance of the partner's gaze fixations relative to its own eyes.[8] Dynamic changes in these gaze-distance variables provide information on the proximity of gaze fixations of interacting individuals to one another. This information becomes particularly valuable for computing interactive gaze events, such as mutual eye contact or joint attention, when gaze-distance variables for self and other converge to specific values. Thus, this parametric representation of gaze-related

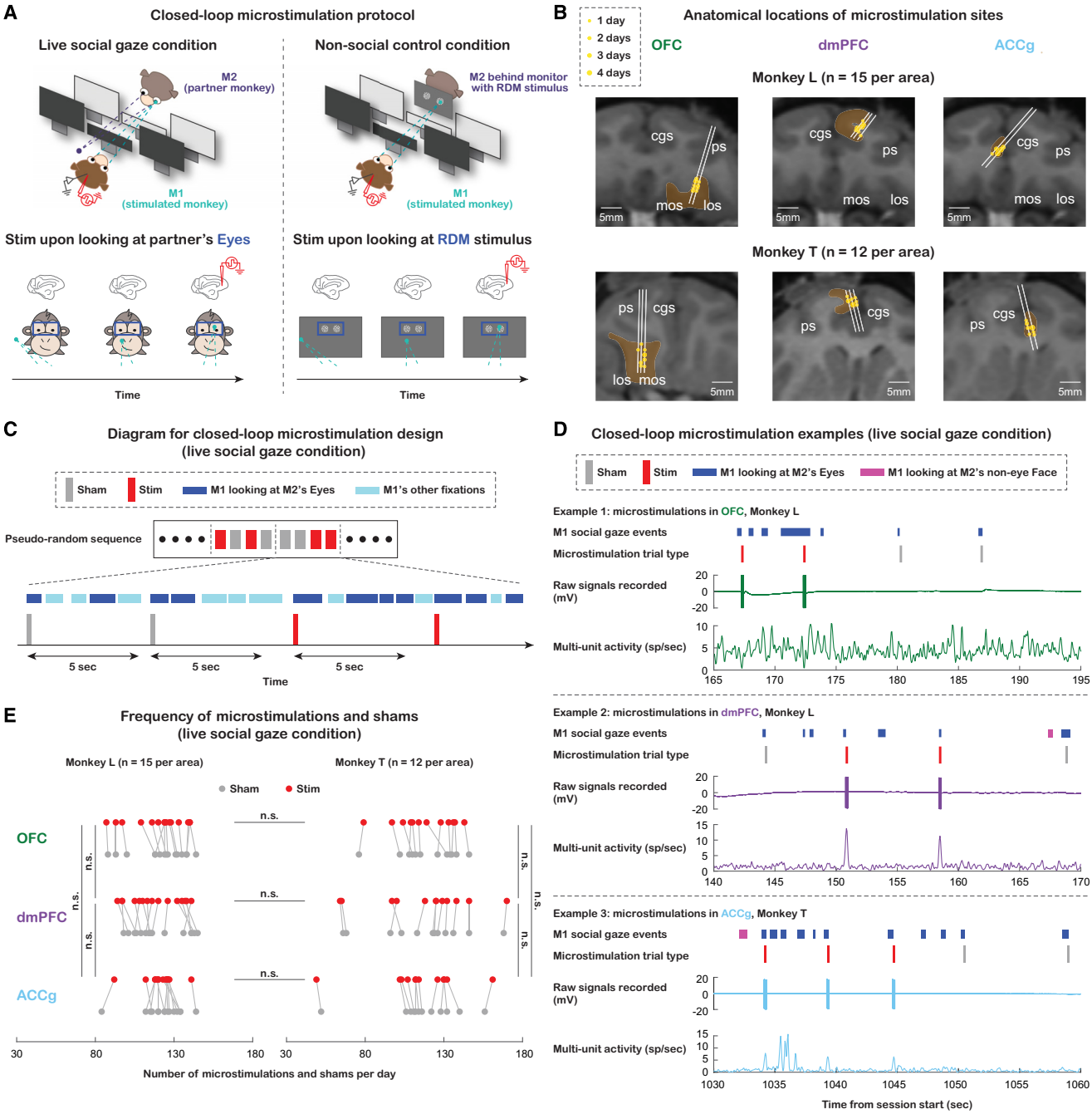

Figure 1. Experimental setup and microstimulation design

(A) Experimental paradigm for studying the functional role of the primate prefrontal cortex in naturalistic social gaze interaction. Left: live social gaze condition where each real-time microstimulation was selectively triggered by M1 fixating on M2's eyes with a probability of 50% (half microstimulation trials and half sham trials). Right: non-social gaze control condition where each real-time microstimulation was selectively triggered by M1 fixating on the random dot motion (RDM) stimulus (same location and size as *eyes* ROI in the live social gaze condition) presented on a mini monitor placed in front of M2's face.

(B) Anatomical localizations of microstimulation sites in the OFC, dmPFC, and ACCg from monkey L (n = 15 per area) and monkey T (n = 12 per area). See Table S1 for the Montreal Neurological Institute (MNI) coordinates of individual microstimulation sites.

(C) Diagram of the closed-loop microstimulation design for the live social gaze condition. To avoid overstimulation of brain tissue, any two consecutive trials (including both microstimulations and shams) had to be at least 5 s apart; for every four trials, two microstimulations and two shams were randomly assigned.

(D) Three examples of 30-s experiment segments from the live social gaze condition. Each example, from top to bottom, shows M1's eyes (blue) and non-eye face (pink) events (other fixations in space are not shown here), shams (gray), and microstimulations (red) triggered by looking at a partner's eyes, raw signals recorded, and multi-unit activity.

(legend continued on next page)

distances in individual OFC, dmPFC, and ACCg neurons is a noteworthy finding as it can provide a moment-by-moment index of social attention during an ongoing social interaction, possibly serving as a simple, yet elegant, mechanism of social gaze monitoring. This type of gaze-distance coding is not specific to social information processing, however. In OFC, it has been shown that a large proportion of neurons encode the gaze fixation distance from a value-predicting cue on the screen during free viewing,[16] providing a potentially shared mechanism linking gaze position and reward valuation in both social and non-social contexts. By contrast, dmPFC is well implicated in mentalizing[17–19] and ACCg has been shown to encode social information in an other-referenced frame.[20–22] Such research findings suggest that the two regions in the primate medial prefrontal cortex could be involved in representing the other's gaze during social interaction.

To address the question whether neural populations in OFC, dmPFC, or ACCg causally contribute to dynamic social attention, here we applied weak, real-time, closed-loop microstimulations unilaterally to each of the three prefrontal areas upon the precise moment when the stimulated monkey fixated on the partner monkey's eyes. Compared with sham stimulations, microstimulations of the OFC facilitated momentary dynamic social attention in the spatial dimension by decreasing the average distance of one's own gaze fixations relative to a partner's eyes. Importantly, this effect was more pronounced for gaze fixations in the contralateral visual field and specific to attending to social stimuli. Moreover, microstimulations of the OFC also exerted an influence in the temporal dimension of social attention by reducing the inter-looking interval for attending to a partner's face as well as reducing the latency to reciprocate a partner's directed gaze. Therefore, microstimulations of the OFC had a dual impact on both spatial and temporal aspects of social attention by facilitating focal visual attention around another social agent and promoting reciprocal gaze exchanges. By contrast, microstimulations of the dmPFC changed how inter-individual gaze dynamics were modulated by one's own gaze positions in space on a longer timescale. These findings highlight the primate OFC as a causal node in controlling momentary social attention while suggesting an involvement of the dmPFC in long-term social gaze exchanges.

RESULTS

Two unique pairs of rhesus macaques (M1: stimulated monkey or "self," monkeys L and T; M2: partner monkey or "other," monkey E) engaged in spontaneous face-to-face social gaze interaction,[8,23] while the gaze positions of both monkeys were continuously and simultaneously tracked at high temporal and spatial resolution. To examine the causal moment-by-moment contributions of different prefrontal areas in live social gaze interaction, we applied weak, real-time, closed-loop microstimulations (75 μA, 100 Hz, 200 ms; STAR Methods; see discussion for more information on microstimulation parameters) with a probability of 50% (half microstimulation trials and half sham trials) contingently upon the moment when the stimulated monkey fixated on the partner monkey's eyes in the live social gaze condition ("eyes stimulation"; Figure 1A, left; Figure S1A; STAR Methods) or on a random dot motion (RDM) stimulus (presented on a mini monitor positioned in front of M2's face) in the non-social control condition (Figure 1A, right). RDM stimulus was chosen as a non-social control because it has no behavioral meaning (i.e., no intrinsic value), yet is still salient to monkeys, and was placed in the same location with the same surrounding visual background as the partner monkey's eyes in the live social gaze condition. Therefore, when comparing between the two conditions, we controlled for the visual angle of fixations on these social and non-social stimuli and prevented attentional competition between the two if presented simultaneously. On each experimental day, microstimulations were applied to one of the three prefrontal areas: OFC, dmPFC, or ACCg (Figure 1B; Table S1). To avoid overstimulation of the brain tissue, any two consecutive trials (including both microstimulation and sham trials) had to be at least 5 s apart; for every four trials, two microstimulations and two shams were randomly assigned (Figures 1C, 1D, S1B, and S1C).

The total number of microstimulations (and shams) received per day was comparable across the three stimulated regions and comparable between the two animals, both in the social gaze and non-social control conditions (Figure 1E, live social gaze condition, all $p > 0.90$, Wilcoxon rank sum, two-sided, false discovery rate [FDR]-corrected; Figure S1D, non-social control condition, all $p > 0.10$). This is important, as we could later rule out the possibility that any observed regional difference or social specificity was simply a result of an unbalanced number of microstimulations received. Similarly, we wanted to ensure that the monkeys' overall attention in an experimental day was comparable across stimulated regions and conditions. We therefore quantified spontaneously occurring gaze behaviors of the stimulated monkeys in the following regions of interest (ROIs): "eyes" and "non-eye face" (the rest of the face excluding the eyes region) of the partner monkey in the live social gaze condition, and the "RDM stimulus" (same location and size as eyes ROI) in the non-social gaze control condition. The total number of fixations on a partner's eyes per day was significantly higher than fixations on non-eye face for all three stimulated brain regions (Figure S1E, top, all $p < 10^{-4}$, Wilcoxon signed rank, two-sided, FDR-corrected), suggesting the significance of gaze directed to eyes that has been shown in previous studies in both humans and nonhuman primates.[8,23–25] In addition, the total number of fixations on a partner's eyes per day was comparable to fixations on the RDM stimulus for days involving the three stimulated regions (Figure S1E, top, all $p > 0.30$), making it reasonable for us to compare the two conditions when examining the

(E) Total number of microstimulations (red) and shams (gray) received per day in the live social gaze condition for monkey L (left) and monkey T (right). Data points connected with lines indicate measurements from the same day. The total number of microstimulations and shams per day was comparable across the three stimulated regions and comparable between the two animals (all $p > 0.90$). n.s., not significant; Wilcoxon rank sum, two-sided, FDR-corrected. Statistics for shams are not shown in the figure; none of the comparisons is significant.
See also Figure S1.

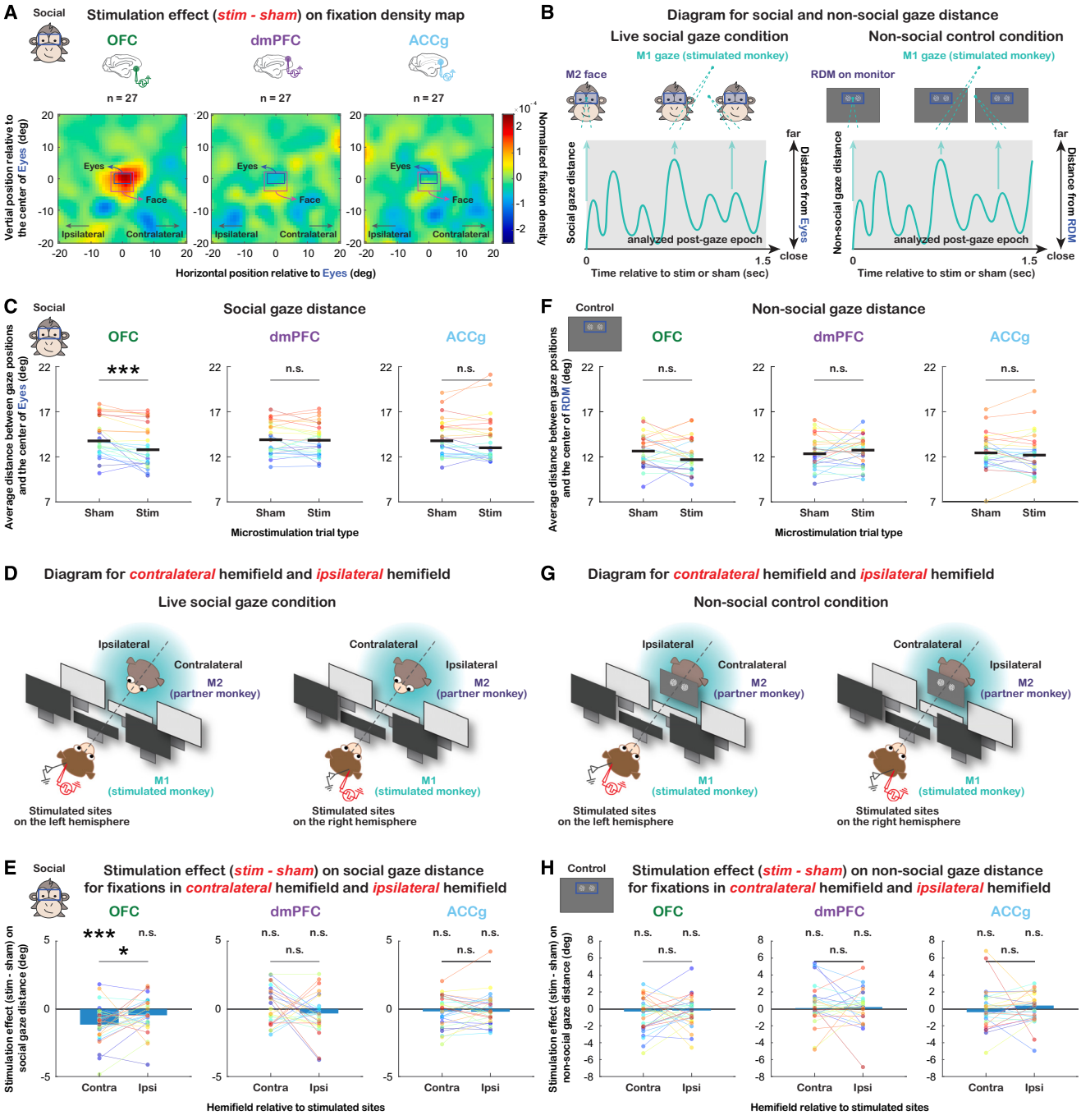

Figure 2. Microstimulation effects on momentary social attention in the spatial dimension

(A) Microstimulation effect (difference between microstimulation and sham trial types) on the fixation density map of space surrounding partner monkey's eyes (blue rectangle) and whole face (pink rectangle) for OFC, dmPFC, and ACCg (n = 27 per area).

(B) Diagrams illustrating social and non-social gaze distances. For each microstimulation or sham, we calculated the average distance of all M1 fixations in space during the analyzed post-gaze epoch (within 1.5 s of the onset of a microstimulation or sham) relative to M2's eyes in the live social gaze condition (social gaze distance, left) and relative to RDM stimulus in the non-social gaze control condition (non-social gaze distance, right).

(C) Average social gaze distance per day (in visual degrees) for sham and microstimulation trial types separately for OFC, dmPFC, and ACCg. Data points in the same color connected with lines indicate measurements from the same day. Compared with shams, microstimulations of the OFC significantly decreased social gaze distance during the post-gaze epoch ($p < 0.001$ for both monkeys combined; this effect was also present and significant in each monkey: $p = 0.008$ for monkey L and $p = 0.002$ for monkey T). ***$p < 0.001$; n.s., not significant; Wilcoxon signed rank, two-sided.

(D) Diagrams illustrating the contralateral hemifield (opposite visual field of the stimulated brain hemisphere) and the ipsilateral hemifield (same visual field as the stimulated brain hemisphere) in the live social gaze condition.

(legend continued on next page)

microstimulation effect as the amount of attention allocated overall was similar.

Closed-loop microstimulations of the OFC facilitate momentary social attention in the spatial dimension

In our prior research, we elucidated a single-cell mechanism of social gaze monitoring in the OFC, dmPFC, and ACCg. Notably, a significant proportion of neurons in these areas exhibited continuous and parametric tracking of where an individual is looking in space relative to another social agent or where the other agent is looking relative to oneself. This finding provides insight into a potential neural mechanism of social gaze monitoring involving these prefrontal regions.[8] The current study investigated whether these prefrontal regions causally regulate such social gaze tracking.

To address this question, we first constructed a fixation density map for each trial, considering all fixations during the analyzed post-gaze epoch (within 1.5 s of the onset of a microstimulation or sham; STAR Methods; supplemental information) in the visual space surrounding the eyes and "whole face" (union of eyes and non-eye face) of the partner monkey. Differences in such fixation density maps between microstimulation and sham trial types revealed a potential role of the OFC in modulating momentary dynamic social attention. Specifically, microstimulations of the OFC led to more clustered subsequent gaze fixations around the partner monkey (Figure 2A; see Figure S2A for the results from individual stimulated monkeys) within this relatively short time window following stimulations. To quantify this momentary effect, for each microstimulation or sham, we calculated the average Euclidean distance between each of the stimulated monkey's gaze fixations during the post-gaze epoch and the center of the partner's eyes in the live social gaze condition (Figure 2B, left, social gaze distance; STAR Methods) or the center of RDM stimulus in the non-social control condition (Figure 2B, right, non-social gaze distance). We then compared the average of these gaze distances per day between microstimulation and sham trial types for each stimulated brain region.

As the fixation density maps show, microstimulations of the OFC significantly decreased the average distance of one's own gaze positions in space relative to a partner's eyes during the post-gaze epoch compared with shams (Figure 2C; $p < 0.001$, Wilcoxon signed rank, two-sided; significant statistics for individual animals are reported in the figure legend; see Figure S2B for an alternative visualization). This suggests a facilitation of social attention in the spatial dimension by promoting gaze fixations around another social agent following OFC microstimulation. By contrast, we did not observe such a stimulation effect on social gaze distance for the dmPFC (Figure 2C, $p = 0.361$) or ACCg (Figure 2C, $p = 0.374$). Notably, the observed stimulation effect of the OFC was more pronounced for gaze fixations in the contralateral visual field of the stimulated brain hemisphere (Figures 2D and 2E; contralateral: $p < 0.001$; significant statistics for individual animals are reported in the figure legend; ipsilateral: $p = 0.068$; contralateral vs. ipsilateral: $p = 0.026$, Wilcoxon signed rank, two-sided). Again, no such effect was observed in either hemifield for the dmPFC (Figure 2E; contralateral: $p = 0.501$; ipsilateral: $p = 0.149$; contralateral vs. ipsilateral: $p = 0.230$) or ACCg (Figure 2E; $p = 0.442$, $p = 0.517$, $p = 0.564$).

Crucially, these stimulation effects of the OFC were exclusively observed in the live social gaze condition (i.e., microstimulations triggered by looking at a partner's eyes) and not in the non-social gaze control condition using the RDM stimulus with no behavioral meaning to monkeys (Figure 2F; OFC: $p = 0.118$; dmPFC: $p = 0.719$; ACCg: $p = 0.302$; Figure S2C). The absence of stimulation effect for the RDM stimulus was also found when gaze fixation locations were split by hemifield for the OFC (Figures 2G and 2H; contralateral: $p = 0.097$; ipsilateral: $p = 0.249$; contralateral vs. ipsilateral: $p = 0.442$), dmPFC ($p = 0.374$; $p = 0.517$; $p = 0.773$) or ACCg ($p = 0.532$; $p = 0.943$; $p = 0.171$), supporting the notion that that the observed effects of OFC microstimulations in the spatial dimension were selective to social gaze interaction or when the stimulus had a behavioral meaning. Separate control experiments ("mouth stimulation"; STAR Methods; supplemental information) revealed that such a microstimulation effect could be further modulated by the specific social gaze events that triggered microstimulations, as we did not observe an effect of OFC microstimulations when they were applied contingently upon looking at the partner monkey's "mouth" region or corresponding RDM stimulus positioned in the same location, unlike what we found for eyes stimulation.

Microstimulations of the OFC also promote momentary social attention in the temporal dimension

Inter-looking interval

In addition to the spatial dimension, the temporal aspect of social attention plays a crucial role in guiding social gaze interaction. Specifically, the time elapsed between individual instances of looking at another agent could serve as an index of social attention, with shorter durations between such gaze events indicating increased social attention. In this context, we sought to determine whether OFC microstimulations contributed to a reduction in the interval between social gaze events in addition to the observed enhancement of social attention in the spatial dimension. Specifically, we examined the latency of M1 to look back at M2's whole face (i.e., the first whole face event within 5 s of the onset of a microstimulation or sham that

(E) Microstimulation effect on social gaze distance for fixations in the contralateral hemifield and ipsilateral hemifield separately for OFC, dmPFC, and ACCg. A negative value here (difference between microstimulation and sham trial types) indicates that microstimulations, compared with shams, resulted in more clustered subsequent gaze fixations around the partner monkey's eyes. Data points in the same color connected with lines indicate measurements from the same day. The observed stimulation effect of the OFC was more pronounced for gaze fixations in the contralateral visual field of the stimulated hemisphere (contralateral: $p < 0.001$ for both monkeys combined; $p = 0.015$ for monkey L and $p = 0.012$ for monkey T; ipsilateral: $p = 0.068$ for both combined; contralateral vs. ipsilateral: $p = 0.026$ for both combined; $p = 0.073$ for L and $p = 0.204$ for T). $^{*}p < 0.05$; $^{***}p < 0.001$; n.s., not significant; Wilcoxon signed rank, two-sided.
(F–H) Same format as (C)–(E) but for the non-social gaze control condition. n.s., not significant; Wilcoxon signed rank, two-sided.
See also Figure S2.

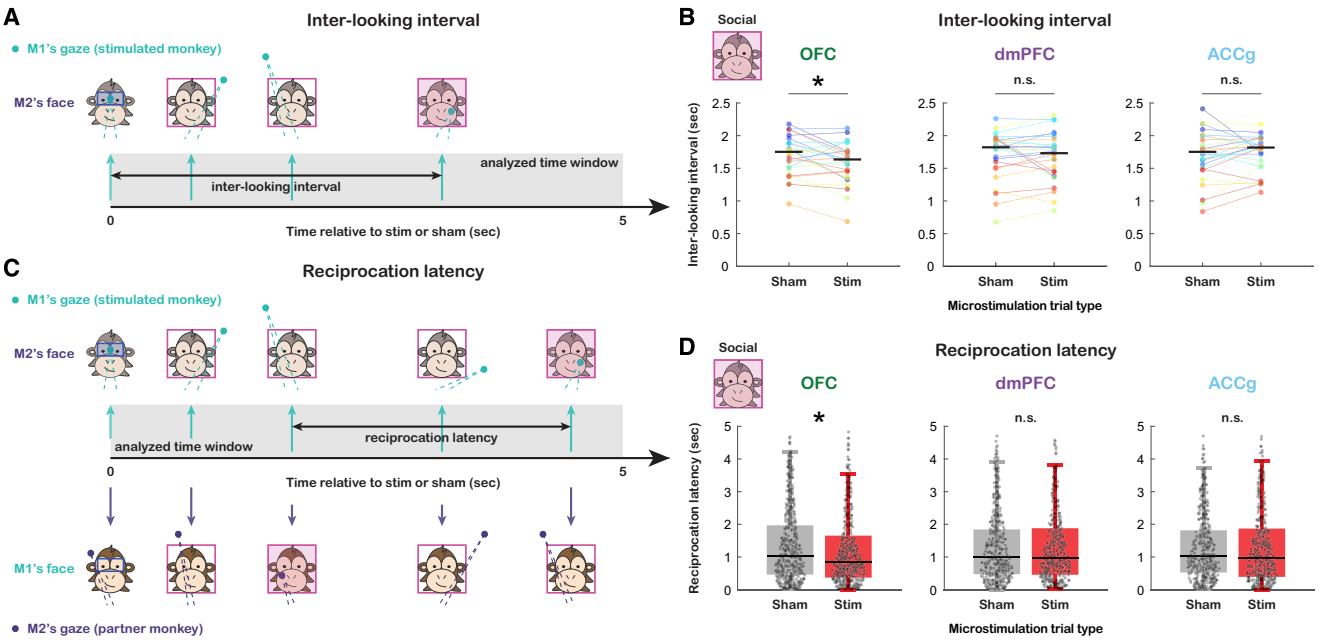

Figure 3. Microstimulation effects on momentary social attention in the temporal dimension

(A) Diagram illustrating inter-looking interval, the latency of M1 to look back at M2's whole face 5 s after the onset of a microstimulation or sham.

(B) Average inter-looking interval per day for sham and microstimulation trial types separately for OFC, dmPFC, and ACCg. Data points in the same color connected with lines indicate measurements from the same day. Microstimulations of the OFC decreased inter-looking interval ($p = 0.035$ for both monkeys combined; $p = 0.188$ for monkey L and $p = 0.092$ for monkey T). *$p < 0.05$; n.s., not significant; Wilcoxon signed rank, two-sided.

(C) Diagram illustrating reciprocation latency, the latency of M1 to gaze back at M2's whole face after M2 looked at M1's whole face during the 5 s after the onset of a microstimulation or sham.

(D) Distribution of reciprocation latency for sham (gray) and microstimulation (red) trial types separately for OFC, dmPFC, and ACCg. Trial-level data were collapsed across all days for each stimulated brain region. Microstimulations of the OFC decreased reciprocation latency ($p = 0.011$ for both combined; $p = 0.074$ for L and $p = 0.079$ for T). *$p < 0.05$; n.s., not significant; Wilcoxon rank sum, two-sided.

See also Figure S3.

was triggered by fixation to a partner's eyes in the live social gaze condition, "inter-looking interval"; Figure 3A; STAR Methods). Microstimulations of the OFC decreased this inter-looking interval (Figure 3B; $p = 0.035$, Wilcoxon signed rank, two-sided; see Figure S3A for an alternative visualization). However, we did not observe such a stimulation effect for the dmPFC (Figure 3B, $p = 0.792$) or ACCg (Figure 3B, $p = 0.291$). Further, this reduction of inter-looking interval from OFC microstimulations was specific to social attention, as no effect was observed in the non-social gaze condition (OFC: $p = 0.773$; dmPFC: $p = 0.080$; ACCg: $p = 0.943$). It is worth noting that this analysis had a relatively low number of relevant gaze events compared with social gaze-distance data from the spatial dimension analysis (i.e., the stimulated monkey did not look back at the partner's whole face during the examined time window on 41% of microstimulation and sham trials per day on average). Nevertheless, when we combined all trials for each stimulated region, we still observed similar results to the day-level analysis above (Figure S3B, OFC: $p = 0.010$; dmPFC: $p = 0.301$; ACCg: $p = 0.602$; Wilcoxon rank sum, two-sided). Microstimulations of the OFC therefore tended to lead monkeys to look back at another social agent faster, which may facilitate social gaze monitoring and dynamic social attention.

Reciprocation latency

We next examined a more explicitly interactive aspect of social gaze dynamics. Specifically, we inspected the average latency of M1 to reciprocate gaze back at M2's whole face after M2 looked at M1's whole face within 5 s of the onset of a microstimulation or sham that was triggered by fixation to the partner's *eyes* ("reciprocation latency"; Figure 3C; STAR Methods). On the day-level, microstimulations did not seem to greatly reduce such reciprocation latency (Figures S3C and S3D, OFC: $p = 0.130$; dmPFC: $p = 0.701$; ACCg: $p = 0.400$; Wilcoxon signed rank, two-sided). However, this is likely due to a low number of relevant gaze events (i.e., there was no sequence of M2 looking at M1 and then M1 looking back at M2 during the examined time window on 86% of microstimulation and sham trials per day on average). When combining all trials for each stimulated region, we observed that microstimulations of the OFC decreased reciprocation latency (Figure 3D; $p = 0.011$, Wilcoxon rank sum, two-sided). We again did not observe such stimulation effect for dmPFC (Figure 3D, $p = 0.777$) or ACCg (Figure 3D, $p = 0.368$). Microstimulations of the OFC therefore tended to lead monkeys to reciprocate another social agent's gaze faster.

Thus, during spontaneous real-life social gaze interaction, closed-loop microstimulations of the OFC, following specific social gaze events, effectively enhanced momentary dynamic

social attention in both spatial and temporal dimensions. In the spatial dimension, the subsequent gaze fixations were more clustered around another social agent, an effect more pronounced in the contralateral hemifield. In the temporal dimension, the inter-looking interval and reciprocation latency were shortened. Crucially, these effects were specific to social attention and were not observed for the RDM stimulus.

Microstimulations do not change momentary social attention in the unstimulated animal

In addition to the stimulated monkey, we also examined the partner monkey's gaze behaviors in response to changes in a stimulated monkey's gaze behaviors due to microstimulations. In the spatial dimension, microstimulations did not change social gaze distance in the partner monkey in any of the regions (OFC: $p = 0.118$; dmPFC: $p = 0.302$; ACCg: $p = 0.064$; Wilcoxon signed rank, two-sided). In the temporal dimension, the definitions of inter-looking interval and reciprocation latency would be different from the partner monkey's perspective compared with the stimulated monkey's perspective. Therefore, we examined the following two latency variables from M2's perspective, inter-looking interval (after M2's gaze event at M1's whole face, the latency of M2 to look back at M1's whole face; i.e., the latency between the second and first whole face events of M2 within 5 s of the onset of a microstimulation or sham) and reciprocation latency (latency of M2 to look at M1's whole face within 5 s of the onset of a microstimulation or sham when M2 was being looked at by M1). Again, microstimulations did not change the inter-looking interval (OFC: $p = 1$; dmPFC: $p = 0.866$; ACCg: $p = 0.249$; Wilcoxon signed rank, two-sided) or reciprocation latency (OFC: $p = 0.665$; dmPFC: $p = 0.773$; ACCg: $p = 0.701$) in the partner monkey in any of the regions. Therefore, we did not find any evidence that the social gaze behaviors of the unstimulated monkey were altered on a short timescale during social gaze interactions.

Do microstimulations of the OFC also lead to longer timescale modulations of social gaze exchanges?

The results reported above have shown that microstimulations of the OFC enhance momentary dynamic social attention within a relatively short time window following stimulations (1.5 s post-gaze epoch). Do these microstimulations also modulate social gaze exchanges on a longer timescale? To examine this, we analyzed inter-individual gaze dynamics between the stimulated monkey and the partner monkey. First, we applied a causal decomposition analysis[26] using moment-by-moment social gaze distance from each monkey (distance between the subject monkey's gaze positions and the center of the other monkey's eyes) during the post-gaze epoch and controlled for saccades (Figures 4A and 4B; STAR Methods). This allowed us to calculate a relative causal strength index that showed how much the gaze behaviors of one monkey in a pair were influenced by the gaze behaviors of the other monkey. To investigate the stimulation effect on a longer timescale, we compared the first 45 stimulations (early epoch) with the next 45 stimulations (late epoch) from each day (STAR Methods). Although microstimulations of the OFC enhanced momentary dynamic social attention, as shown in the previous sections, they did not seem to impact gaze directionality, indexed by the magnitude of relative causal strength for both time epochs combined (Figure S4A; $p = 0.239$, Wilcoxon signed rank, two-sided) and for each epoch separately (Figure S4B, all $p > 0.16$). Further, to examine whether inter-individual gaze dynamics were modulated by where the stimulated monkey was looking in space, we correlated social gaze distance and relative causal strength (STAR Methods) and found the slope of this fitted correlation comparable between early and late epochs for the OFC (Figure S4C, both hemifields combined: $p = 0.757$; Figure 4C, contralateral: $p = 0.882$; Figure S4D, ipsilateral: $p = 0.098$).

However, the slope of this fitted correlation for dmPFC was stronger for the late epoch than early epoch, specifically for gaze fixations in the contralateral hemifield (Figure 4D; $p = 0.015$, permutation test; Figure S4E, both hemifields combined: $p = 0.131$; Figure S4F, ipsilateral: $p = 0.455$). These results suggested that microstimulations of the dmPFC, but not of the OFC or ACCg, altered how social gaze exchanges were modulated by the location of the stimulated monkey's gaze fixations in space on a longer timescale. Specifically, the slope of this examined correlation on average was positive in both early and late epochs for gaze fixations in both hemifields for dmPFC, indicating that as the stimulated monkey fixated closer around the partner monkey (smaller social gaze distance), his gaze behaviors were more likely to be led by the partner (lower relative causal strength). Intriguingly, as the number of dmPFC microstimulations accumulated within an experiment day, this effect became larger (greater slope for late epoch compared with early epoch). Microstimulations of the dmPFC therefore altered how social gaze exchanges were modulated by the location of the subject's gaze fixations on a relatively long timescale.

Microstimulation effects of the OFC and dmPFC are not driven by low-level properties of saccades

Importantly, the observed effects of OFC and dmPFC microstimulations were not driven by any change in the duration of the current looking into a partner's eyes that triggered a microstimulation or sham (Figure 5A, OFC: $p = 0.302$; dmPFC: $p = 0.269$; Wilcoxon signed rank, two-sided), pupil size (Figure 5B, no time bin was significant; Wilcoxon signed rank, two-sided), number of microsaccades (Figure 5C, OFC: $p = 0.456$; dmPFC: $p = 0.581$; Wilcoxon signed rank, two-sided), number of macrosaccades (Figure 5D, OFC: $p = 0.055$; dmPFC: $p = 0.230$), macrosaccade peak velocity (Figure 5E, OFC: $p = 0.848$; dmPFC: $p = 1$), macrosaccade kinematics indexed by saccade peak velocity over amplitude (Figure 5F, OFC: $p = 0.665$; dmPFC: $p = 0.904$; Wilcoxon signed rank, two-sided; Figure 5G, OFC: $p = 0.515$; dmPFC: $p = 0.164$; permutation test), or macrosaccade kinematics when considering saccade direction (Figure 5H, II: macrosaccades from the ipsilateral hemifield to the ipsilateral hemifield; IC: macrosaccades from the ipsilateral hemifield to the contralateral hemifield; CI; CC; OFC: all $p > 0.47$; dmPFC: all $p > 0.31$; Wilcoxon signed rank, two-sided).

DISCUSSION

In primates, the gaze serves a critical function as they navigate through their social environment. Our previous

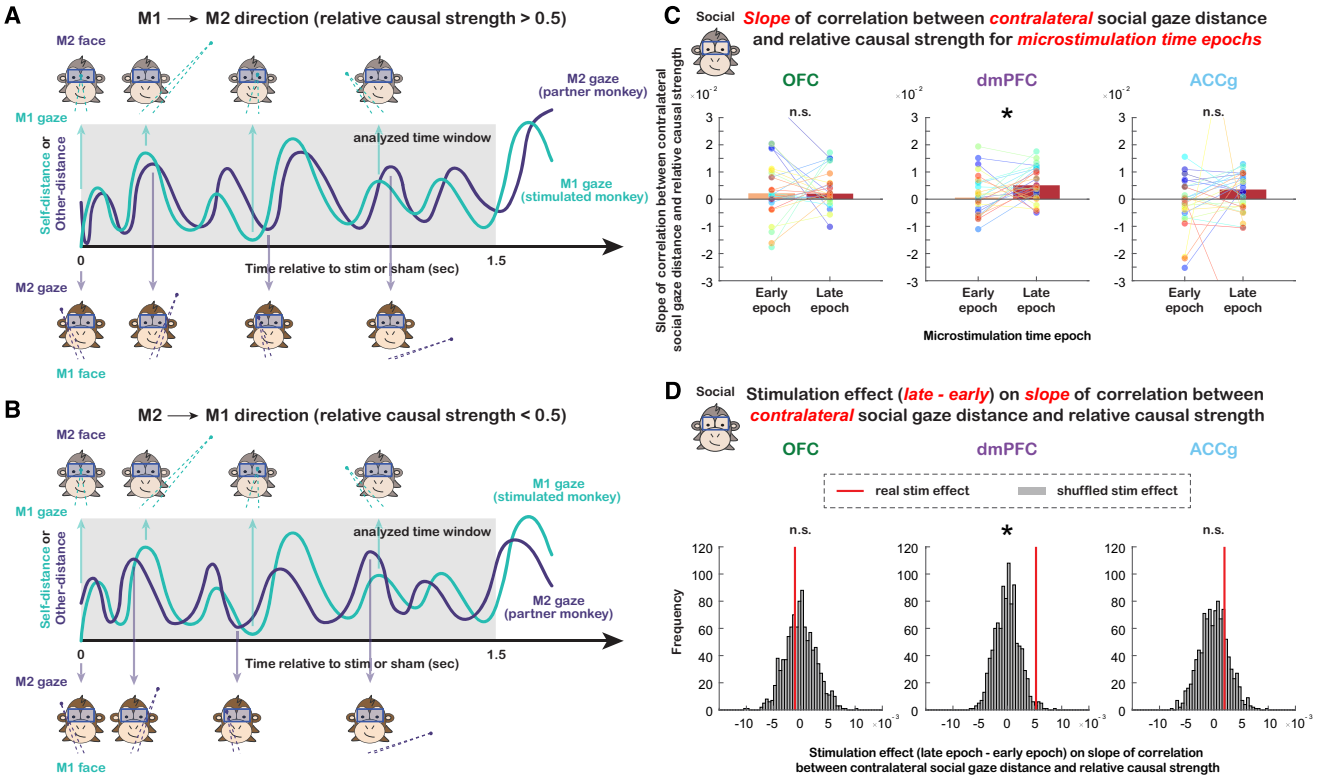

Figure 4. Longer timescale microstimulation effects on social gaze exchanges

(A) Diagram for M1 to M2 social gaze directionality when relative causal strength was greater than 0.5.

(B) Diagram for M2 to M1 social gaze directionality when relative causal strength was less than 0.5.

(C) Slope of correlation between social gaze distance in the contralateral hemifield and relative causal strength for microstimulations in the early epoch and late epoch separately for OFC, dmPFC, and ACCg. Data points in the same color connected with lines indicate measurements from the same day. For dmPFC, the slope of this fitted correlation was stronger for the late epoch than early epoch ($p = 0.054$ for both monkeys combined; $p = 0.048$ for monkey L and $p = 0.625$ for monkey T). *$p \approx 0.05$; n.s., not significant; Wilcoxon signed rank, two-sided.

(D) Microstimulation effect (difference between late and early time epochs) on the slope of examined correlation in (C). Red lines show the real median slope difference between late epoch and early epoch, whereas gray bars show the shuffled null distribution of slope difference medians (shuffling time epoch label 1,000 times for each day). The slope of this fitted correlation was stronger for the late epoch than early epoch for the dmPFC when using gaze fixations in the contralateral hemifield ($p = 0.015$ for both combined; $p = 0.038$ for L and $p = 0.068$ for T). *$p < 0.05$; n.s., not significant; permutation test.

See also Figure S4.

electrophysiological work revealed that interactive social gaze variables are widely represented in the primate prefrontal-amygdala networks. In addition to the amygdala, a substantial proportion of neurons in the OFC, dmPFC, and ACCg represent key signatures of social gaze interaction. Notably, spiking activity of many neurons in these prefrontal regions parametrically tracks the individual's own gaze relative to another agent ("social gaze distance" also examined in the current paper) as well as the other agent's gaze relative to the subject.[8] Here, we report that weak, real-time, closed-loop microstimulations of the OFC modulate momentary dynamic social attention. In the spatial dimension, these microstimulations resulted in clustered subsequent gaze fixations around another agent (reduced social gaze distance), an effect more pronounced for gaze fixations in the contralateral hemifield. In the temporal dimension, these microstimulations reduced the inter-looking interval for attending to another agent and the latency to reciprocate the other's directed gaze. These effects were found to be occurring on a relatively short timescale, as OFC microstimulations did not change how long-term social gaze exchanges were modulated by the location of the subject's own gaze fixations, unlike what we found with dmPFC microstimulations.

Widespread representations of social gaze variables in the OFC, dmPFC, and ACCg neurons[8] are likely shaped by their common anatomical connectivity patterns with other brain regions in the social brain.[5] The three prefrontal regions, albeit to different degrees, are bidirectionally connected to the amygdala,[27–30] often referred to as the hub of social cognition[31,32] and implicated in both face and gaze processing.[8,33–35] These shared functionalities might be enabled by widespread projections from the basolateral amygdala (BLA) to these brain regions, defining multiple networks between BLA and frontal cortical areas.[36] Moreover, the orbitofrontal and medial prefrontal cortices, including the regions examined in this study, receive innervation from subregions in the inferior temporal (IT) cortex and the superior temporal sulcus (STS).[37–39] These anatomical connections are likely to be functionally important for social gaze processing. The primate IT contains multiple face

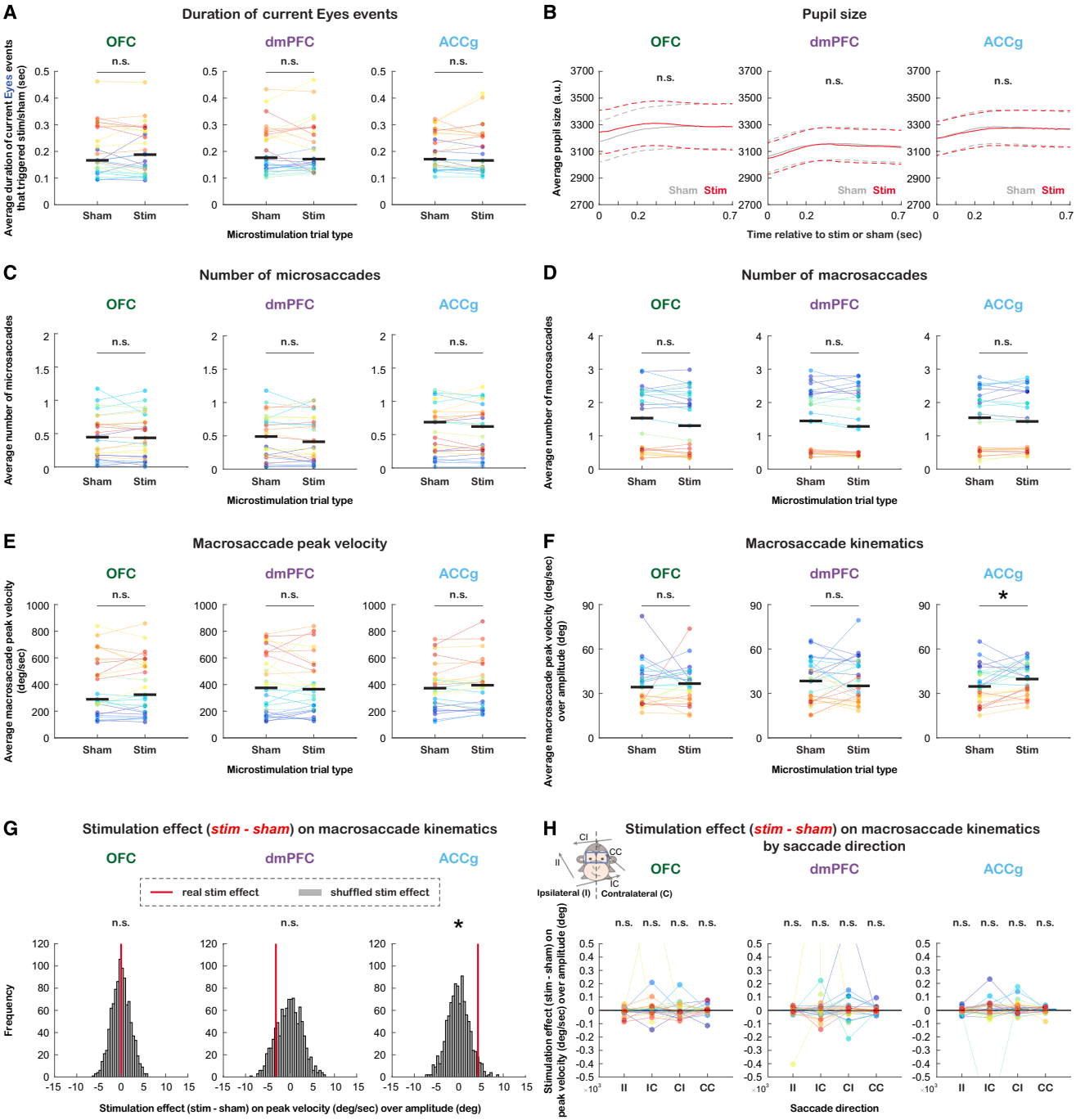

Figure 5. Control analyses on current gaze events, pupil size, and saccades

(A) Average duration per day of current eyes events that triggered a microstimulation or sham, for sham and microstimulation trial types separately for OFC, dmPFC, and ACCg. Data points in the same color connected with lines indicate measurements from the same day. n.s., not significant; Wilcoxon signed rank, two-sided.

(B) Average pupil size aligned to trial onset for sham (gray) and microstimulation (red) trial types for OFC, dmPFC, and ACCg. Solid lines indicate the mean while the dotted lines indicate the standard error of the mean (SEM). No difference was observed for pupil size between the two trial types throughout the 700-ms period following trial onset for any of the three stimulated regions. n.s., not significant; Wilcoxon signed rank, two-sided.

(C and D) Average number of microsaccades (C) and macrosaccades (D) per day during post-gaze epoch for the two trial types separately for OFC, dmPFC, and ACCg. n.s., not significant; Wilcoxon signed rank, two-sided.

(E) Average macrosaccade peak velocity for the two trial types separately for OFC, dmPFC, and ACCg. n.s., not significant; Wilcoxon signed rank, two-sided.

(legend continued on next page)

patches[40–42] and the middle STS is believed to be a potential macaque homolog of the human temporal parietal junction, implicated in mentalizing in humans,[43] based on both functional connectivity[44] and neural recoding.[45] Face processing and mentalizing functions might be closely intertwined with the representations of social gaze variables. With regard to this notion, it is possible that the interactive social gaze signals in the OFC, dmPFC, and ACCg are subserving more abstract social cognitive functions that are functionally shared with social gaze processing.

During social gaze interaction, individuals constantly evaluate objects and other individuals in the environment and make momentary decisions to look toward or away from them. OFC neurons encode a wide range of outcome-related variables, such as expected value, choice value, reward prediction error, and choice and outcome history[46–48] that dynamically contribute to value and decision computations in OFC populations.[49–51] These decision computations in the OFC might facilitate the encoding of moment-to-moment value associated with the other's gaze and looking at the other's eyes for guiding adaptive behaviors. Indeed, value coding in OFC neurons is known to be modulated by gaze location. When monkeys freely viewed reward-predicting cues presented on a monitor, value signals in many OFC cells associated with the cues increased when monkeys fixated closer to the cues,[16] suggesting a crucial role of the OFC in both valuation and attention, two components also foundational to social gaze interaction. It has also been shown that, in the OFC, weak microstimulations, similar to the ones used here, enhanced value computations during decision-making.[48] Taken together, this might suggest a possible mechanism for the observed effects of OFC microstimulations. We hypothesize that weak, closed-loop microstimulations of the OFC would increase the value signals associated with certain social gaze events and therefore enhance subsequent social attention.

It has long been theorized that looking at the face or the eyes of a conspecific has adaptive value.[52] Indeed, value and social gaze variables have been shown to be representationally shared in the primate amygdala,[53] which is strongly reciprocally connected to OFC.[30] Our findings might reflect a synergistic effect of the intrinsic value of social stimuli and microstimulation. The face and eyes are highly valued and readily capture attention. Weak microstimulations could further amplify the value signals in the OFC[48] associated with looking at a social agent, thereby driving monkeys to fixate closer to and attend faster to the agent. Importantly, the effects of OFC microstimulations we observed were specific to the social context and not observed in the non-social control condition. This is likely because the RDM stimulus does not have any intrinsic or adaptive value in our experimental context, although it is visually salient and captures attention. In addition, in our separate mouth stimulation control experiments, where microstimulations with exactly the same parameters were applied contingently upon looking at a partner's mouth region or corresponding RDM stimulus, we did not observe an effect of OFC microstimulations. It is interesting to note that, in our experimental setting, monkeys almost never made vocalizations or facial expressions involving salient mouth movements and, therefore, our observed effects specific to eyes stimulation might be guided by where the most salient, informative, and dynamic information was observable. For the same reason, we anticipate that OFC microstimulations could enhance attention to certain non-social objects when they hold adaptive value, such as bananas, or learned cues that predict reward[16] or that guide gaze-following.[12]

Studies that have causally manipulated activity in the primate brain have provided critical insights into brain functions. Microstimulations of the face patches in IT revealed their interconnectivity and distorted face perception.[54,55] Microstimulations of a gaze-following patch in the posterior STS impaired gaze-following behaviors when monkeys viewed images with different gaze directions.[12,13] In the decision-making literature, microstimulations of the OFC were shown to bias choices[48] and disrupt value comparison.[56] Further, closed-loop microstimulations of the OFC delivered contingently upon theta frequency oscillation were shown to disrupt this synchronization and impair reward-guided learning.[57] In this study, closed-loop microstimulations of the OFC delivered upon specific social gaze events enhanced momentary social attention.

Intriguingly, we also found that microstimulations of the dmPFC altered how social gaze exchanges were modulated by the location of the subject's gaze fixations on a longer timescale. The closer the stimulated monkey looked near the partner monkey, the more likely his gaze behaviors were led by the partner. Based on the hypothesized role of dmPFC in mentalizing and representing social information about self and other,[18,58–60] this finding is consistent with the possibility that dmPFC microstimulations might have modulated the computations for understanding the intention of the other's gaze, which likely requires building an internal model of a social agent over multiple interactive bouts between self and other on a longer timescale. It also agrees with the argument that the dmPFC represents interpersonal relationships and causal links between environmental features, including social environment.[61] On the other hand, we observed neither short-term nor long-term microstimulation effect in the ACCg. Given that social gaze signals are widely found in the OFC, dmPFC, and ACCg,[8] such dissociated functional consequences among the three areas from our closed-loop microstimulation protocol suggest potential differentiations on how microstimulations affect different prefrontal populations. However, the current study cannot rule out whether evoking behavioral changes in different neural tissues may require tailored

(F) Average macrosaccade kinematics per day indexed by saccade peak velocity over amplitude for the two trial types separately for OFC, dmPFC, and ACCg. *$p < 0.05$; n.s., not significant; Wilcoxon signed rank, two-sided.
(G) Microstimulation effect (difference between microstimulation and sham trial types) on macrosaccade kinematics. Red lines show the real median stimulation effect, whereas gray bars show the shuffled null distribution (shuffling microstimulation trial type label 1,000 times for each day). *$p < 0.05$, permutation test.
(H) Microstimulation effect on macrosaccade kinematics by saccade direction separately for OFC, dmPFC, and ACCg. II: macrosaccades from the ipsilateral hemifield to the ipsilateral hemifield; IC: macrosaccades from the ipsilateral hemifield to the contralateral hemifield; CI; CC. n.s., not significant; Wilcoxon signed rank, two-sided.

stimulation protocols or parameters. For example, given its specialization in encoding social information referenced to others,[21,22,62,63] microstimulations applied upon specific gaze events of the partner monkey might reveal a causal involvement of ACCg in social gaze interaction.

It is critical for future studies to explore the stimulation parameter space, as effects of different brain areas could depend on the choice of parameters.[48,56] In our current work, we referred to the microstimulation literature and chose frequency and duration (100 Hz and 200 ms) that fall within the range of commonly used parameters.[64–66] Microstimulation amplitude seems to play a more complicated role, however. Previous studies overall suggest that low or medium stimulation amplitude typically enhances brain function, while high-amplitude stimulation ($\geq$100 μA) typically disrupts brain function. For example, low-amplitude pulses biased monkeys to perceive motion encoded by the stimulated neurons, whereas with high-amplitude pulses, monkeys no longer distinguished motion direction.[65] Similarly, high-amplitude microstimulations of face patches in monkey IT led to distortion of face perception,[54] again suggesting function impairment due to high-amplitude stimulations. More relevant to our stimulated prefrontal regions, low-amplitude microstimulation (25, 50 μA) of the OFC increased subjective value, whereas high-amplitude microstimulation ($\geq$100 μA) disrupted value-guided decision-making in monkeys.[48] However, it is important to note that our reference to these studies was largely based on observed behavioral changes induced by stimulations as these studies did not directly examine the neural activation vs. inhibition effects from these cortical microstimulations. Thus, we were unable to interpret our results directly from the perspectives of the stimulated neural populations. In general, the exact mapping between cortical microstimulation parameters and underlying neural activation patterns is not well understood.

Nevertheless, there is some agreement that low-frequency and low-amplitude stimulations could increase firing rate through synaptic transmission,[67–70] whereas high-frequency and high-amplitude stimulation could shut down neural activity due to "neural hijacking" when the natural neural activity becomes blocked or replaced by stimulus-evoked firing activity that leads to disrupted processing.[71,72] Although the exact stimulation parameters within which such a mechanism transition happens likely depend on the specific stimulated brain regions and their induced behavioral changes,[69,72–75] our microstimulation parameters are more in line with a function-enhancing mechanism. Moreover, while our study focused on a closed-loop microstimulation protocol because we were interested in precisely linking each behavioral gaze event to each microstimulation, and we hoped to better control for the monkey's gaze position when a microstimulation was applied, future work should test non-closed-loop microstimulation to examine whether our findings could extend to a more general stimulation protocol.

In the current study, with a goal to first determine the causal contribution of the OFC, dmPFC, and ACCg in dynamic social attention, we did not systematically manipulate the social relationship between the pairs of monkeys involved. Instead, we controlled for familiarity and sex variables, as our tested animals were consistently familiar male-female pairs with the same female partner. However, social gaze dynamics can be influenced by social factors such as dominance, familiarity, and sex.[23] The orbitofrontal and medial prefrontal networks are also differentially connected to a specific region in the temporal pole[76] that processes personally familiar faces.[77] Therefore, future work is needed to examine how our observed effects of the OFC and dmPFC microstimulations on dynamic social attention might be influenced by social relationships. Furthermore, our stimulation sites in the dmPFC and ACCg covered multiple subregions. However, our unbalanced samples from these subregions prevented us from examining their potential difference in microstimulation effect that would be important to investigate in future studies.

During ongoing gaze exchanges, it is critical to dynamically increase or decrease attention to another social agent following specific social gaze events. Such behavioral contingency or adaptability is essential in guiding social interaction. Moreover, given the importance of social gaze in multitudes of social behaviors in primate species, social gaze representations in the brain may be tightly coupled to action- or outcome-related information about other social agents that is critical for observational learning and social decision-making.[18,22,59,78] Importantly, atypical visual attention and social gaze patterns are frequently associated with social disorders, such as autism spectrum disorder (ASD).[79–82] Our findings also have a therapeutic implication for using closed-loop microstimulation protocols—a "social brain interface"—to modulate atypical social attention and social gaze behaviors in ASD. Stimulating OFC during an eye looking training session may help improve momentary social attention, and stimulating the dmPFC could potentially enhance responsiveness in social gaze exchanges on a longer timescale. Future investigations utilizing a noninvasive closed-loop stimulation protocol will help develop therapeutics to mitigate atypical social gaze behaviors.

STAR★METHODS

Detailed methods are provided in the online version of this paper and include the following:

- KEY RESOURCES TABLE
- RESOURCE AVAILABILITY
  - Lead contact
  - Materials availability
  - Data and code availability
- EXPERIMENTAL MODEL AND SUBJECT DETAILS
  - Animals
- METHOD DETAILS
  - Experimental setup
  - Surgery and anatomical localization
  - Closed-loop microstimulation protocol
- QUANTIFICATION AND STATISTICAL ANALYSIS
  - Frequency of microstimulations and regions of interest for social and non-social gaze sessions
  - Fixation density map
  - Gaze distance analyses
  - Gaze distance analyses (Mouth stimulation)
  - Gaze latency analyses
  - Inter-individual gaze dynamics analyses
  - Control analyses on current gaze events, pupil size, and saccades

SUPPLEMENTAL INFORMATION

Supplemental information can be found online at https://doi.org/10.1016/j.neuron.2024.05.004.

ACKNOWLEDGMENTS

This work was supported by the National Institute of Mental Health (R01MH110750, R01MH120081, and R01 MH128190).

AUTHOR CONTRIBUTIONS

S.W.C.C., S.F., and O.D.M. designed the study and wrote the paper. S.F., A.R.N., and O.D.M. performed the experiments. S.F., N.A.F., O.D.M., and S.W.C.C. analyzed the data.

DECLARATION OF INTERESTS

The authors declare no competing interests.

Received: January 1, 2024
Revised: April 11, 2024
Accepted: May 6, 2024
Published: May 31, 2024

REFERENCES

1. Passingham, R.E., and Wise, S.P. (2012). The Neurobiology of the Prefrontal Cortex: Anatomy, Evolution, and the Origin of Insight (Oxford University Press). https://doi.org/10.1093/acprof:osobl/9780199552917.001.0001.
2. Chang, S.W.C., Brent, L.J.N., Adams, G.K., Klein, J.T., Pearson, J.M., Watson, K.K., and Platt, M.L. (2013). Neuroethology of primate social behavior. Proc. Natl. Acad. Sci. USA *110*, 10387–10394. https://doi.org/10.1073/pnas.1301213110.
3. Sliwa, J., and Freiwald, W.A. (2017). A dedicated network for social interaction processing in the primate brain. Science *356*, 745–749. https://doi.org/10.1126/science.aam6383.
4. Wittmann, M.K., Lockwood, P.L., and Rushworth, M.F.S. (2018). Neural Mechanisms of Social Cognition in Primates. Annu. Rev. Neurosci. *41*, 99–118. https://doi.org/10.1146/annurev-neuro-080317-061450.
5. Gangopadhyay, P., Chawla, M., Dal Monte, O., and Chang, S.W.C. (2021). Prefrontal-amygdala circuits in social decision-making. Nat. Neurosci. *24*, 5–18. https://doi.org/10.1038/s41593-020-00738-9.
6. Mitani, J.C., Call, J., Kappeler, P.M., Palombit, R.A., and Silk, J.B. (2012). The evolution of primate societies (University of Chicago Press).
7. Shepherd, S.V., and Freiwald, W.A. (2018). Functional Networks for Social Communication in the Macaque Monkey. Neuron *99*, 413–420.e3. https://doi.org/10.1016/j.neuron.2018.06.027.
8. Dal Monte, O., Fan, S., Fagan, N.A., Chu, C.J., Zhou, M.B., Putnam, P.T., Nair, A.R., and Chang, S.W.C. (2022). Widespread implementations of interactive social gaze neurons in the primate prefrontal-amygdala networks. Neuron *110*, 2183–2197.e7. https://doi.org/10.1016/j.neuron.2022.04.013.
9. Perrett, D.I., Hietanen, J.K., Oram, M.W., and Benson, P.J. (1992). Organization and Functions of Cells Responsive to Faces in the Temporal Cortex [and Discussion]. Philos. Trans.: Biol. Sci. *335*, 23–30. https://doi.org/10.1098/rstb.1992.0003.
10. Roy, A., Shepherd, S.V., and Platt, M.L. (2014). Reversible inactivation of pSTS suppresses social gaze following in the macaque (Macaca mulatta). Soc. Cogn. Affect. Neurosci. *9*, 209–217. https://doi.org/10.1093/scan/nss123.
11. De Souza, W.C., Eifuku, S., Tamura, R., Nishijo, H., and Ono, T. (2005). Differential characteristics of face neuron responses within the anterior superior temporal sulcus of macaques. J. Neurophysiol. *94*, 1252–1266. https://doi.org/10.1152/jn.00949.2004.
12. Ramezanpour, H., and Thier, P. (2020). Decoding of the other's focus of attention by a temporal cortex module. Proc. Natl. Acad. Sci. USA. *117*, 2663–2670. https://doi.org/10.1073/pnas.1911269117.
13. Chong, I., Ramezanpour, H., and Thier, P. (2023). Causal manipulation of gaze-following in the macaque temporal cortex. Prog. Neurobiol. *226*, 102466. https://doi.org/10.1016/j.pneurobio.2023.102466.
14. Nummenmaa, L., and Calder, A.J. (2009). Neural mechanisms of social attention. Trends Cogn. Sci. *13*, 135–143. https://doi.org/10.1016/j.tics.2008.12.006.
15. Itier, R.J., and Batty, M. (2009). Neural bases of eye and gaze processing: the core of social cognition. Neurosci. Biobehav. Rev. *33*, 843–863. https://doi.org/10.1016/j.neubiorev.2009.02.004.
16. McGinty, V.B., Rangel, A., and Newsome, W.T. (2016). Orbitofrontal Cortex Value Signals Depend on Fixation Location during Free Viewing. Neuron *90*, 1299–1311. https://doi.org/10.1016/j.neuron.2016.04.045.
17. Yoshida, K., Saito, N., Iriki, A., and Isoda, M. (2011). Representation of others' action by neurons in monkey medial frontal cortex. Curr. Biol. *21*, 249–253. https://doi.org/10.1016/j.cub.2011.01.004.
18. Yoshida, K., Saito, N., Iriki, A., and Isoda, M. (2012). Social error monitoring in macaque frontal cortex. Nat. Neurosci. *15*, 1307–1312. https://doi.org/10.1038/nn.3180.
19. Isoda, M., Noritake, A., and Ninomiya, T. (2018). Development of social systems neuroscience using macaques. Proc. Jpn. Acad. Ser. B Phys. Biol. Sci. *94*, 305–323. https://doi.org/10.2183/pjab.94.020.
20. Apps, M.A.J., and Ramnani, N. (2014). The Anterior Cingulate Gyrus Signals the Net Value of Others' Rewards. J. Neurosci. *34*, 6190–6200. https://doi.org/10.1523/jneurosci.2701-13.2014.
21. Apps, M.A., Rushworth, M.F., and Chang, S.W. (2016). The Anterior Cingulate Gyrus and Social Cognition: Tracking the Motivation of Others. Neuron *90*, 692–707. https://doi.org/10.1016/j.neuron.2016.04.018.
22. Chang, S.W., Gariépy, J.F., and Platt, M.L. (2013). Neuronal reference frames for social decisions in primate frontal cortex. Nat. Neurosci. *16*, 243–250. https://doi.org/10.1038/nn.3287.
23. Dal Monte, O., Piva, M., Morris, J.A., and Chang, S.W. (2016). Live interaction distinctively shapes social gaze dynamics in rhesus macaques. J. Neurophysiol. *116*, 1626–1643. https://doi.org/10.1152/jn.00442.2016.
24. Kano, F., Shepherd, S.V., Hirata, S., and Call, J. (2018). Primate social attention: Species differences and effects of individual experience in humans, great apes, and macaques. PLoS One *13*, e0193283. https://doi.org/10.1371/journal.pone.0193283.
25. Gothard, K.M., Erickson, C.A., and Amaral, D.G. (2004). How do rhesus monkeys (Macaca mulatta) scan faces in a visual paired comparison task? Anim. Cogn. *7*, 25–36. https://doi.org/10.1007/s10071-003-0179-6.
26. Yang, A.C., Peng, C.-K., and Huang, N.E. (2018). Causal decomposition in the mutual causation system. Nat. Commun. *9*, 3378. https://doi.org/10.1038/s41467-018-05845-7.
27. Vogt, B.A., and Pandya, D.N. (1987). Cingulate cortex of the rhesus monkey: II. Cortical afferents. J. Comp. Neurol. *262*, 271–289. https://doi.org/10.1002/cne.902620208.
28. Morecraft, R.J., Geula, C., and Mesulam, M.M. (1992). Cytoarchitecture and neural afferents of orbitofrontal cortex in the brain of the monkey. J. Comp. Neurol. *323*, 341–358. https://doi.org/10.1002/cne.903230304.
29. Amaral, D.G., and Price, J.L. (1984). Amygdalo-cortical projections in the monkey (Macaca fascicularis). J. Comp. Neurol. *230*, 465–496. https://doi.org/10.1002/cne.902300402.
30. Carmichael, S.T., and Price, J.L. (1995). Limbic connections of the orbital and medial prefrontal cortex in macaque monkeys. J. Comp. Neurol. *363*, 615–641. https://doi.org/10.1002/cne.903630408.
31. Bickart, K.C., Dickerson, B.C., and Barrett, L.F. (2014). The amygdala as a hub in brain networks that support social life. Neuropsychologia *63*, 235–248. https://doi.org/10.1016/j.neuropsychologia.2014.08.013.
32. Putnam, P.T., and Chang, S.W.C. (2021). Toward a holistic view of value and social processing in the amygdala: Insights from primate behavioral neurophysiology. Behav. Brain Res. *411*, 113356. https://doi.org/10.1016/j.bbr.2021.113356.

33. Gothard, K.M., Battaglia, F.P., Erickson, C.A., Spitler, K.M., and Amaral, D.G. (2007). Neural responses to facial expression and face identity in the monkey amygdala. J. Neurophysiol. *97*, 1671–1683. https://doi.org/10.1152/jn.00714.2006.

34. Mosher, C.P., Zimmerman, P.E., and Gothard, K.M. (2014). Neurons in the monkey amygdala detect eye contact during naturalistic social interactions. Curr. Biol. *24*, 2459–2464. https://doi.org/10.1016/j.cub.2014.08.063.

35. Taubert, J., Flessert, M., Wardle, S.G., Basile, B.M., Murphy, A.P., Murray, E.A., and Ungerleider, L.G. (2018). Amygdala lesions eliminate viewing preferences for faces in rhesus monkeys. Proc. Natl. Acad. Sci. USA. *115*, 8043–8048. https://doi.org/10.1073/pnas.1807245115.

36. Zeisler, Z.R., London, L., Janssen, W.G., Fredericks, J.M., Elorette, C., Fujimoto, A., Zhan, H., Russ, B.E., Clem, R.L., Hof, P.R., et al. (2023). Single basolateral amygdala neurons in macaques exhibit distinct connectional motifs with frontal cortex. Neuron *111*, 3307–3320.e5. https://doi.org/10.1016/j.neuron.2023.09.024.

37. Seltzer, B., and Pandya, D.N. (1989). Frontal lobe connections of the superior temporal sulcus in the rhesus monkey. J. Comp. Neurol. *281*, 97–113. https://doi.org/10.1002/cne.902810108.

38. Borra, E., and Luppino, G. (2017). Functional anatomy of the macaque temporo-parieto-frontal connectivity. Cortex *97*, 306–326. https://doi.org/10.1016/j.cortex.2016.12.007.

39. Ungerleider, L.G., Gaffan, D., and Pelak, V.S. (1989). Projections from inferior temporal cortex to prefrontal cortex via the uncinate fascicle in rhesus monkeys. Exp. Brain Res. *76*, 473–484. https://doi.org/10.1007/bf00248903.

40. Tsao, D.Y., Moeller, S., and Freiwald, W.A. (2008). Comparing face patch systems in macaques and humans. Proc. Natl. Acad. Sci. USA *105*, 19514–19519. https://doi.org/10.1073/pnas.0809662105.

41. Tsao, D.Y., Freiwald, W.A., Tootell, R.B., and Livingstone, M.S. (2006). A cortical region consisting entirely of face-selective cells. Science *311*, 670–674. https://doi.org/10.1126/science.1119983.

42. Park, S.H., Koyano, K.W., Russ, B.E., Waidmann, E.N., McMahon, D.B.T., and Leopold, D.A. (2022). Parallel functional subnetworks embedded in the macaque face patch system. Sci. Adv. *8*, eabm2054. https://doi.org/10.1126/sciadv.abm2054.

43. Frith, U., and Frith, C.D. (2003). Development and neurophysiology of mentalizing. Philos. Trans. R. Soc. Lond. B Biol. Sci. *358*, 459–473. https://doi.org/10.1098/rstb.2002.1218.

44. Mars, R.B., Sallet, J., Neubert, F.-X., and Rushworth, M.F.S. (2013). Connectivity profiles reveal the relationship between brain areas for social cognition in human and monkey temporoparietal cortex. Proc. Natl. Acad. Sci. USA *110*, 10806–10811. https://doi.org/10.1073/pnas.1302956110.

45. Ong, W.S., Madlon-Kay, S., and Platt, M.L. (2021). Neuronal correlates of strategic cooperation in monkeys. Nat. Neurosci. *24*, 116–128. https://doi.org/10.1038/s41593-020-00746-9.

46. Padoa-Schioppa, C., and Assad, J.A. (2006). Neurons in the orbitofrontal cortex encode economic value. Nature *441*, 223–226. https://doi.org/10.1038/nature04676.

47. Hunt, L.T., Malalasekera, W.M.N., de Berker, A.O., Miranda, B., Farmer, S.F., Behrens, T.E.J., and Kennerley, S.W. (2018). Triple dissociation of attention and decision computations across prefrontal cortex. Nat. Neurosci. *21*, 1471–1481. https://doi.org/10.1038/s41593-018-0239-5.

48. Ballesta, S., Shi, W., Conen, K.E., and Padoa-Schioppa, C. (2020). Values encoded in orbitofrontal cortex are causally related to economic choices. Nature *588*, 450–453. https://doi.org/10.1038/s41586-020-2880-x.

49. Rich, E.L., and Wallis, J.D. (2016). Decoding subjective decisions from orbitofrontal cortex. Nat. Neurosci. *19*, 973–980. https://doi.org/10.1038/nn.4320.

50. Chiang, F.K., Wallis, J.D., and Rich, E.L. (2022). Cognitive strategies shift information from single neurons to populations in prefrontal cortex. Neuron *110*, 709–721.e4. https://doi.org/10.1016/j.neuron.2021.11.021.

51. McGinty, V.B., and Lupkin, S.M. (2023). Behavioral read-out from population value signals in primate orbitofrontal cortex. Nat. Neurosci. *26*, 2203–2212. https://doi.org/10.1038/s41593-023-01473-7.

52. Emery, N.J. (2000). The eyes have it: the neuroethology, function and evolution of social gaze. Neurosci. Biobehav. Rev. *24*, 581–604. https://doi.org/10.1016/s0149-7634(00)00025-7.

53. Pryluk, R., Shohat, Y., Morozov, A., Friedman, D., Taub, A.H., and Paz, R. (2020). Shared yet dissociable neural codes across eye gaze, valence and expectation. Nature *586*, 95–100. https://doi.org/10.1038/s41586-020-2740-8.

54. Moeller, S., Crapse, T., Chang, L., and Tsao, D.Y. (2017). The effect of face patch microstimulation on perception of faces and objects. Nat. Neurosci. *20*, 743–752. https://doi.org/10.1038/nn.4527.

55. Moeller, S., Freiwald, W.A., and Tsao, D.Y. (2008). Patches with links: a unified system for processing faces in the macaque temporal lobe. Science *320*, 1355–1359. https://doi.org/10.1126/science.1157436.

56. Ballesta, S., Shi, W., and Padoa-Schioppa, C. (2022). Orbitofrontal cortex contributes to the comparison of values underlying economic choices. Nat. Commun. *13*, 4405. https://doi.org/10.1038/s41467-022-32199-y.

57. Knudsen, E.B., and Wallis, J.D. (2020). Closed-Loop Theta Stimulation in the Orbitofrontal Cortex Prevents Reward-Based Learning. Neuron *106*, 537–547.e4. https://doi.org/10.1016/j.neuron.2020.02.003.

58. Falcone, R., Cirillo, R., Ferraina, S., and Genovesio, A. (2017). Neural activity in macaque medial frontal cortex represents others' choices. Sci. Rep. *7*, 12663. https://doi.org/10.1038/s41598-017-12822-5.

59. Noritake, A., Ninomiya, T., and Isoda, M. (2018). Social reward monitoring and valuation in the macaque brain. Nat. Neurosci. *21*, 1452–1462. https://doi.org/10.1038/s41593-018-0229-7.

60. Báez-Mendoza, R., Mastrobattista, E.P., Wang, A.J., and Williams, Z.M. (2021). Social agent identity cells in the prefrontal cortex of interacting groups of primates. Science *374*, eabb4149. https://doi.org/10.1126/science.abb4149.

61. Klein-Flügge, M.C., Bongioanni, A., and Rushworth, M.F.S. (2022). Medial and orbital frontal cortex in decision-making and flexible behavior. Neuron *110*, 2743–2770. https://doi.org/10.1016/j.neuron.2022.05.022.

62. Behrens, T.E.J., Hunt, L.T., Woolrich, M.W., and Rushworth, M.F.S. (2008). Associative learning of social value. Nature *456*, 245–249. https://doi.org/10.1038/nature07538.

63. Basile, B.M., Schafroth, J.L., Karaskiewicz, C.L., Chang, S.W.C., and Murray, E.A. (2020). The anterior cingulate cortex is necessary for forming prosocial preferences from vicarious reinforcement in monkeys. PLoS Biol. *18*, e3000677. https://doi.org/10.1371/journal.pbio.3000677.

64. Salzman, C.D., Britten, K.H., and Newsome, W.T. (1990). Cortical microstimulation influences perceptual judgements of motion direction. Nature *346*, 174–177. https://doi.org/10.1038/346174a0.

65. Murasugi, C.M., Salzman, C.D., and Newsome, W.T. (1993). Microstimulation in visual area MT: effects of varying pulse amplitude and frequency. J. Neurosci. *13*, 1719–1729. https://doi.org/10.1523/jneurosci.13-04-01719.1993.

66. Moore, T., and Fallah, M. (2004). Microstimulation of the Frontal Eye Field and Its Effects on Covert Spatial Attention. J. Neurophysiol. *91*, 152–162. https://doi.org/10.1152/jn.00741.2002.

67. Stoney, S.D., Jr., Thompson, W.D., and Asanuma, H. (1968). Excitation of pyramidal tract cells by intracortical microstimulation: effective extent of stimulating current. J. Neurophysiol. *31*, 659–669. https://doi.org/10.1152/jn.1968.31.5.659.

68. Salzman, C.D., Murasugi, C.M., Britten, K.H., and Newsome, W.T. (1992). Microstimulation in visual area MT: effects on direction discrimination performance. J. Neurosci. *12*, 2331–2355. https://doi.org/10.1523/jneurosci.12-06-02331.1992.

69. Ethier, C., Brizzi, L., Darling, W.G., and Capaday, C. (2006). Linear summation of cat motor cortex outputs. J. Neurosci. *26*, 5574–5581. https://doi.org/10.1523/jneurosci.5332-05.2006.

70. Histed, M.H., Bonin, V., and Reid, R.C. (2009). Direct activation of sparse, distributed populations of cortical neurons by electrical microstimulation. Neuron *63*, 508–522. https://doi.org/10.1016/j.neuron.2009.07.016.

71. Griffin, D.M., Hudson, H.M., Belhaj-Saïf, A., and Cheney, P.D. (2011). Hijacking Cortical Motor Output with Repetitive Microstimulation. J. Neurosci. *31*, 13088–13096. https://doi.org/10.1523/jneurosci.6322-10.2011.

72. Van Acker, G.M., 3rd, Amundsen, S.L., Messamore, W.G., Zhang, H.Y., Luchies, C.W., Kovac, A., and Cheney, P.D. (2013). Effective intracortical microstimulation parameters applied to primary motor cortex for evoking forelimb movements to stable spatial end points. J. Neurophysiol. *110*, 1180–1189. https://doi.org/10.1152/jn.00172.2012.

73. Tehovnik, E.J., and Sommer, M.A. (1997). Electrically evoked saccades from the dorsomedial frontal cortex and frontal eye fields: a parametric evaluation reveals differences between areas. Exp. Brain Res. *117*, 369–378. https://doi.org/10.1007/s002210050231.

74. Thier, P., and Andersen, R.A. (1998). Electrical microstimulation distinguishes distinct saccade-related areas in the posterior parietal cortex. J. Neurophysiol. *80*, 1713–1735. https://doi.org/10.1152/jn.1998.80.4.1713.

75. Graziano, M.S., Taylor, C.S., and Moore, T. (2002). Complex movements evoked by microstimulation of precentral cortex. Neuron *34*, 841–851. https://doi.org/10.1016/s0896-6273(02)00698-0.

76. Kondo, H., Saleem, K.S., and Price, J.L. (2003). Differential connections of the temporal pole with the orbital and medial prefrontal networks in macaque monkeys. J. Comp. Neurol. *465*, 499–523. https://doi.org/10.1002/cne.10842.

77. Landi, S.M., and Freiwald, W.A. (2017). Two areas for familiar face recognition in the primate brain. Science *357*, 591–595. https://doi.org/10.1126/science.aan1139.

78. Azzi, J.C.B., Sirigu, A., and Duhamel, J.-R. (2012). Modulation of value representation by social context in the primate orbitofrontal cortex. Proc. Natl. Acad. Sci. USA *109*, 2126–2131. https://doi.org/10.1073/pnas.1111715109.

79. Klin, A., Jones, W., Schultz, R., Volkmar, F., and Cohen, D. (2002). Visual fixation patterns during viewing of naturalistic social situations as predictors of social competence in individuals with autism. Arch. Gen. Psychiatry *59*, 809–816. https://doi.org/10.1001/archpsyc.59.9.809.

80. Dalton, K.M., Nacewicz, B.M., Johnstone, T., Schaefer, H.S., Gernsbacher, M.A., Goldsmith, H.H., Alexander, A.L., and Davidson, R.J. (2005). Gaze fixation and the neural circuitry of face processing in autism. Nat. Neurosci. *8*, 519–526. https://doi.org/10.1038/nn1421.

81. Dawson, G., Webb, S.J., and McPartland, J. (2005). Understanding the nature of face processing impairment in autism: insights from behavioral and electrophysiological studies. Dev. Neuropsychol. *27*, 403–424. https://doi.org/10.1207/s15326942dn2703_6.

82. Wang, S., Jiang, M., Duchesne, X.M., Laugeson, E.A., Kennedy, D.P., Adolphs, R., and Zhao, Q. (2015). Atypical Visual Saliency in Autism Spectrum Disorder Quantified through Model-Based Eye Tracking. Neuron *88*, 604–616. https://doi.org/10.1016/j.neuron.2015.09.042.

83. Fedorov, A., Beichel, R., Kalpathy-Cramer, J., Finet, J., Fillion-Robin, J.C., Pujol, S., Bauer, C., Jennings, D., Fennessy, F., Sonka, M., et al. (2012). 3D Slicer as an image computing platform for the Quantitative Imaging Network. Magn. Reson. Imaging *30*, 1323–1341. https://doi.org/10.1016/j.mri.2012.05.001.

84. Chakravarty, M., Frey, S., and Collins, L. (2008). Digital atlas of the rhesus monkey brain in stereotaxic coordinates. Rhesus Monkey Brain Stereotaxic Coordinates, pp. 403–407.

85. Frey, S., Pandya, D.N., Chakravarty, M.M., Petrides, M., and Collins, D.L. (2009). MNI monkey space. Neurosci. Res. *65*, S130.

86. Frey, S., Pandya, D.N., Chakravarty, M.M., Bailey, L., Petrides, M., and Collins, D.L. (2011). An MRI based average macaque monkey stereotaxic atlas and space (MNI monkey space). Neuroimage *55*, 1435–1442. https://doi.org/10.1016/j.neuroimage.2011.01.040.

87. Brainard, D.H. (1997). The Psychophysics Toolbox. Spat. Vis. *10*, 433–436. https://doi.org/10.1163/156856897X00357.

88. Cornelissen, F.W., Peters, E.M., and Palmer, J. (2002). The Eyelink Toolbox: Eye tracking with MATLAB and the Psychophysics Toolbox. Behav. Res. Methods Instrum. Comput. *34*, 613–617. https://doi.org/10.3758/BF03195489.

89. Krassanakis, V., Filippakopoulou, V., and Nakos, B. (2014). EyeMMV toolbox: An eye movement post-analysis tool based on a two-step spatial dispersion threshold for fixation identification. J. Eye Mov. Res. *7*, 1–10. https://doi.org/10.16910/jemr.7.1.1.

90. Otero-Millan, J., Castro, J.L.A., Macknik, S.L., and Martinez-Conde, S. (2014). Unsupervised clustering method to detect microsaccades. J. Vision *14*, 18. https://doi.org/10.1167/14.2.18.

91. Paxinos, G., Petrides, M., Huang, X.F., and Toga, A.W. (2008). The Rhesus Monkey Brain in Stereotaxic Coordinates (Elsevier Science).

STAR★METHODS

KEY RESOURCES TABLE

REAGENT or RESOURCE	SOURCE	IDENTIFIER
Critical commercial assays		
Eye tracking camera	SR Research	EyeLink 1000
Headpost	Grey Matter Research	N/A
Recording chamber	Crist and Rogue Research Inc.	N/A
Recording electrodes	FHC Inc.	N/A
Stimulation electrodes	FHC Inc.	N/A
Multi-electrode Microdrive system	NaN Instruments	N/A
Neural recording data acquisition system	Plexon OmniPlex system	N/A
Microstimulation system	PlexStim Electrical Stimulator System	N/A
Deposited data		
Behavioral and neural data	This paper	https://doi.org/10.5281/zenodo.11110157 https://dandiarchive.org/dandiset/000959
Experimental models: organisms/strains		
Macaca mulatta monkeys	N/A	N/A
Software and algorithms		
MATLAB	Mathworks	2017a–2022a
3D Slicer	Fedorov et al.[83]	https://www.slicer.org
MNI rhesus macaque atlas	Chakravarty et al.,[84] Frey et al.,[85] and Frey et al.[86]	https://www.bic.mni.mcgill.ca/ServicesAtlases/Rhesus
Psychtoolbox	Brainard[87]	http://psychtoolbox.org/
EyeLink toolbox	Cornelissen et al.[88]	http://psychtoolbox.org/docs/EyelinkToolbox
Variable coherence random dot motion library	Shadlen lab	https://shadlenlab.columbia.edu/resources/VCRDM.html)
EyeMMV toolbox	Krassanakis et al.[89]	https://github.com/krasvas/EyeMMV
Microsaccade detection software	Otero-Millan et al.[90]	http://smc.neuralcorrelate.com/sw/microsaccade-detection/
Causal decomposition analysis	Yang et al.[26]	https://github.com/accyang/causal-decomposition-analysis
Codes	This paper	https://doi.org/10.5281/zenodo.11110139 https://github.com/changlabneuro/microstim-ofc-social-attention

RESOURCE AVAILABILITY

Lead contact

Further information and requests for resources and reagents should be directed to and will be fulfilled by the lead contact, Steve W.C. Chang (steve.chang@yale.edu).

Materials availability

This study did not generate new unique reagents.

Data and code availability

Behavioral and neural data presented in this paper are available through the DANDI archive (https://dandiarchive.org/dandiset/000959) and the main analysis codes are available at https://github.com/changlabneuro/microstim-ofc-social-attention.

EXPERIMENTAL MODEL AND SUBJECT DETAILS

Animals

Two adult male rhesus macaques (*Macaca mulatta*) were involved as stimulated monkeys (M1; monkeys L and T; both aged 10 years, weighing 15.7 kg and 14.1 kg, respectively). For each M1, unrelated monkey E (female, aged 10 years, weighing 10.9 kg) served as a partner monkey (M2). M2 was previously housed in the same colony room with M1s and other rhesus macaques and later moved to an adjacent colony room. Both pairs had been involved in similar social gaze interaction sessions in previous studies from the lab[8,23] and therefore they were familiar with each other. The focus of this current study was to first investigate the causal functions of OFC, dmPFC, and ACCg in dynamic social attention, so we did not systematically manipulate the social relationship between the pairs of monkeys, but instead consistently chose familiar male-female pairs as our tested animals. Our previous published work using the identical paradigm has provided a comprehensive examination of the effects of social relationship on social gaze interaction from unique 8 dominance-related, 20 familiarity-related, and 20 sex-related perspectives.[23] Here, we did not have the necessary number of pairs to examine the effects of social relationships. It is thus an important future direction to investigate if and how microstimulation effects might be modulated by such social factors. In this study, all animals were kept on a 12-hr light/dark cycle with unrestricted access to food, but controlled access to fluid during testing. All procedures were approved by the Yale Institutional Animal Care and Use Committee and in compliance with the National Institutes of Health Guide for the Care and Use of Laboratory Animals. No animals were excluded from our analyses.

METHOD DETAILS

Experimental setup

On each day, M1 and M2 sat in primate chairs (Precision Engineering, Inc.) facing each other, 100 cm apart and the top of each monkey's head 75 cm from the floor, with three monitors facing each monkey and the middle monitor 36 cm away from each monkey's eyes (Figures 1A and S1A). Two infrared eye-tracking cameras (EyeLink 1000, SR Research) simultaneously and continuously recorded the horizontal and vertical eye positions from both monkeys at 1,000 Hz. We conducted a two-step calibration procedure described in our previous work.[8]

Each data collection day consisted of a total of alternating 10 "live social gaze" sessions and 5 "non-social control" sessions on average for monkey L (9-11 social and 4-8 control sessions across all days) and alternating 15 live social gaze sessions and 5 non-social control sessions on average for monkey T (14-15 social and 5 control sessions across all days). Each session lasted 300 sec. During live social gaze sessions, pairs of monkeys were allowed to freely interact with each other using gaze (Figure 1A, left). During non-social control sessions, M1 was allowed to freely examine the space where a random dot motion (RDM) stimulus was presented on a mini monitor positioned on M2's primate chair directly in front of M2's face (Figure 1A, right). At the beginning of each live social gaze session, the middle monitors were lowered down remotely so that the two monkeys could fully see each other (Figure 1A, top; Figure S1A). Before the beginning of each non-social control session, the mini monitor was positioned by an experimenter in front of M2's face (Figure 1A, right) and the middle monitors were lowered down remotely once the experimenter left the testing room. The mini monitor was 38 cm x 21 cm (W x H) at a resolution of 1024 pixel x 768 pixel. RDM stimulus was constructed using Variable Coherence Random Dot Motion MATLAB library (https://shadlenlab.columbia.edu/resources/VCRDM.html) and contained randomly moving dots within two circular apertures of 2.4 deg diameter each, with an inter-aperture horizontal distance of 1.6 deg equidistantly placed to the left and right of the center of M2's Eyes ROI. RDM stimulus (white dots on a black background, with a density of 16.7 dots/deg^2 per second) generated apparent motion either upward or downward with a 100% coherence with a fixed velocity 2 deg/sec. Motion direction remained consistent within a session. At the end of each session, the middle monitors were raised up remotely and blocked the stimulated monkey's visual access to the partner monkey or the RDM stimulus during a 180-sec break.

Surgery and anatomical localization

All animals received a surgically implanted headpost (Grey Matter Research) for restraining their head movement. A second surgery was performed on the two M1 animals to implant a custom chamber (Rogue Research Inc.) to permit recording and microstimulation in OFC (13), dmPFC (8 and 9), and ACCg (24a, 24b, and 32).[91] Placement of the chambers was guided by both structural magnetic resonance imaging (MRI, 3T Siemens) scans and stereotaxic coordinates. See Figure 1B for microstimulation sites overlayed on representative MR slices from both monkeys. Individual stimulated monkey's MRI was registered to a Montreal Neurological Institute (MNI) rhesus macaque atlas[84–86] by using SlicerANTs extension in 3D Slicer software.[83] See Table S1 for the MNI coordinates of individual microstimulation sites.

Closed-loop microstimulation protocol

On each day before data collection, a guide tube was used to penetrate intact dura and to guide a microstimulation electrode (median impedance 50 kΩ, FHC Inc.) and a recording electrode (tungsten, FHC Inc.), which were remotely lowered by using a motorized multi-electrode microdrive system (NaN Instruments) at the speed of 0.02 mm/sec. After the two electrodes reached target site, we ensured that we positioned the electrodes in the grey matter and waited 30 min for the tissue to settle for signal stability before starting experiment. The microstimulation site was usually positioned within 1mm from the recording electrode site on the chamber grid.

In our main experiments (Eyes stimulation; n = 15 per area from monkey L and n = 12 per area from monkey T), each closed-loop microstimulation (PlexStim system, Plexon Inc.) was triggered immediately upon the detection of a fixation within M2's Eyes region in the live social gaze condition or within the RDM stimulus region (same location and size as Eyes ROI) in the non-social control condition, with a probability of 50%. To accomplish this closed-loop microstimulation protocol, M1's gaze positions were continuously tracked by using an infrared eye-tracking camera (EyeLink 1000, SR Research) at 1,000 Hz and monitored by using an Arduino and custom software. Our software directly digitized the analog output from the eye tracker and monitored in real-time (i.e., with < 1 msec of latency) whether M1's gaze position was inside or outside the targeted ROI. In order to detect fixations online, our software maintained a continuously updating history of the previous 150-msec of M1's gaze positions. A fixation was registered when the maximum dispersion in this time interval was less than 1 visual degree. In this way, a microstimulation (or sham) could be triggered when M1 was determined to be both fixating (based on the online definition of fixation described above) and currently within the targeted ROI. All of these were implemented in real-time and our closed-loop microstimulation protocol allowed the application of microstimulations and shams to be fully dependent on M1's spontaneous gaze behaviors and therefore did not require any manual input. In separate control experiments (Mouth stimulation; n = 5 per area from monkey T), microstimulations with exactly the same parameters were applied contingently upon M1 looking within M2's Mouth region or corresponding RDM stimulus (same location and size as Mouth ROI). Psychtoolbox[87] and EyeLink toolbox[88] were used for analyses.

Specifically, parameters of each microstimulation (cathode-leading bipolar with a phase duration of 200 μsec and an interphase duration of 100 μsec) were 75 μA in amplitude, 100 Hz in frequency, and 200 msec in duration (see discussion for more information on microstimulation parameters). To avoid overstimulation of brain tissue, any two consecutive trials (including both microstimulations and shams) had to be at least 5 sec apart; for every four trials, two microstimulations and two shams were randomly assigned (Figures 1C, 1D, S1B, and S1C).

QUANTIFICATION AND STATISTICAL ANALYSIS

Frequency of microstimulations and regions of interest for social and non-social gaze sessions

To quantify the frequency of microstimulations received by the stimulated monkeys, we calculated and compared the total number of microstimulations and shams per day across the three stimulated brain regions and two animals by using Wilcoxon rank sum test. The comparable frequency across stimulated regions and animals both in the social gaze condition (Figure 1E) and non-social control condition (Figure S1D) allowed us to later rule out the possibility that any observed regional difference or social specificity was simply a result of an unbalanced number of microstimulations received.

In our main Eyes stimulation experiments, on each day, we identified the following regions of interest (ROIs): Eyes and non-eye Face (the rest of the face excluding the Eyes regions) in the live social gaze condition, and RDM stimulus in the non-social control condition (same location and size as Eyes ROI). In some analyses, we examined whole Face which is the union of Eyes and non-eye Face ROIs. Based on each day's calibration, whole Face ROI was defined by the four corners of a monkey's face and the Eyes ROI was defined by adding a padding of $\frac{7}{24}$ (width of the face − distance between the two eyes) to the center of each eye. Fixations were identified using EyeMMV toolbox in MATLAB.[89] We detected fixations based on spatial and duration parameters, using t1 = 1.18 and t2 = 0.59 degrees of visual angle for the spatial tolerances and a minimum duration of 70 msec. For each of the ROIs, we calculated the total number of gaze fixations and the average duration per fixation of the stimulated monkey for each day. Wilcoxon signed rank test was used to compare each variable between Eyes and non-eye Face, as well as Eyes and RDM stimulus. Wilcoxon rank sum test was used to compare each variable of each ROI between any pair of stimulated brain regions. Our results showed that M1's overall attention was comparable across stimulated regions and conditions (Figure S1E). In our Mouth stimulation control experiments, we identified a Mouth ROI that was the same size as Eyes ROI without padding and centered on the mouth region based on each day's calibration. Corresponding RDM stimulus (same location and size as Mouth ROI) was presented on a mini monitor positioned on M2's primate chair directly in front of M2's face.

Fixation density map

To construct a fixation density map, we examined the gaze positions of all M1's fixations in space during the post-gaze epoch (within 1.5 sec after the onset of a microstimulation or sham) and assigned each fixation to a one-visual degree grid-square in a big spatial grid spanning 40 deg in both horizontal and vertical dimensions centered on partner's Eyes ROI. Total number of fixations per day was calculated by summing across such fixations in each grid-square for microstimulation trials and sham trials separately and were z-scored. Difference in such fixation density between microstimulation and sham trial types was averaged across days for each stimulated brain region and plotted as heatmaps aligned to the center of partner's Eyes (Figure 2A, monkey T's heatmaps were flipped horizontally as his chamber was implanted on the different hemisphere as monkey L; see Figure S2A for individual stimulated animals).

Gaze distance analyses

In the live social gaze condition, for each trial, we examined all M1's fixations during post-gaze epoch and calculated the Euclidean distance between each fixation and the center of partner's Eyes ROI projected onto the same plane. Such distance was first averaged across all fixations after each trial and then averaged for each trial type for each day (Figure 2B). Wilcoxon signed rank test was used

to compare social gaze distance between microstimulation and sham trial types (Figure 2C; see Figure S2B for an alternative visualization). We focused on the post-gaze epoch (within 1.5 sec after the onset of a microstimulation or sham) because it was the common time window for both animals where we observed a significant decrease in social gaze distance following OFC microstimulations. In fact, the effect was present and lasted longer beyond 1.5 sec in one of the stimulated monkeys (within 2 sec after trial onset: $p = 0.003$ for both monkeys combined; $p = 0.008$ for monkey L and $p = 0.204$ for monkey T; within 3 sec: $p = 0.004$ for both combined; $p = 0.007$ for L and $p = 0.204$ for T; Wilcoxon signed rank, two-sided). Fixations were further categorized into those in the contralateral hemifield (opposite visual field of the stimulated brain hemisphere; Figure 2D) and ipsilateral hemifield (same visual field as the stimulated brain hemisphere) for each M1 separately. The microstimulation effect on social gaze distance was examined for fixations in the contralateral and ipsilateral hemifield separately (Figure 2E). Wilcoxon signed rank test was used to compare microstimulation effect on social gaze distance for each hemifield separately and between hemifields. The same analysis was applied for the non-social control condition (Figures 2F–2H and S2C) by calculating the Euclidean distance between M1's fixations and the center of RDM stimulus.

In addition to looking at social gaze distance in a continuous manner, we also examined fixations based on a binary definition (i.e., a fixation was within an ROI or not). Following OFC microstimulations, unlike more clustered subsequent gaze fixations around another social agent, we did not observe any change in the total number of fixations within partner's Eyes (within 1.5 sec: $p > 0.18$ for both monkey L and monkey T; within 2 sec: $p > 0.24$; within 3 sec: $p > 0.30$; Wilcoxon signed rank, two-sided) or whole Face (within 1.5 sec: $p > 0.12$; within 2 sec: $p > 0.20$; within 3 sec: $p > 0.22$), suggesting that the enhanced social attention from OFC microstimulations was driven by having spatially closer gaze fixations around another social agent but not necessarily increased the number of fixations within the social agent's eyes or face regions. However, this conclusion could be limited to the closed-loop microstimulation paradigm and to our specific stimulation parameters (i.e., microstimulations with a different set of parameters might be able to increase the frequency of subsequent gaze fixations back to partner's Eyes). In addition, we applied the criterion such that any two consecutive trials had to be at least 5 sec apart to avoid overstimulation of the brain tissue. This criterion also limited the number of microstimulations or shams that monkeys could potentially receive per day. As we examined a fixed time period following a microstimulation or sham, the duration of fixations also mattered. The longer a fixation within the Eyes was, the less likely the monkey would have a subsequent fixation within the Eyes again. We thus also examined the total duration of fixations during the post-gaze epoch. With OFC microstimulations, the monkeys spent more time looking within the partner's whole Face ($p = 0.003$, stim minus sham difference = 48.9 msec for both monkeys combined; $p = 0.008$, diff = 66.6 msec for monkey L and $p = 0.129$, diff = 39.5 msec for monkey T). Although this effect was not significant in monkey T, the effect was in the expected direction and stronger for microstimulations of OFC compared to the other two regions (dmPFC: $p = 0.683$, diff = -14.5 msec for both combined; $p = 0.639$, diff = -14.5 msec for L and $p = 1$, diff = -5.7 msec for T; ACCg: $p = 0.848$, diff = 3.4 msec for both combined; $p = 0.330$, diff = 16.9 msec for L and $p = 0.677$, diff = 26.6 msec for T). Similar results were observed for total duration of fixations within partner's Eyes albeit weaker (OFC: $p = 0.044$, diff = 16.5 msec for both combined; $p = 0.121$, diff = 16.5 msec for L and $p = 0.233$, diff = 9.4 msec for T). Therefore, it is possible that the longer duration of looking within partner's Eyes or whole Face prevented an increased number of fixations as described above when examining the post-gaze epoch.

Gaze distance analyses (Mouth stimulation)

Similarly, for Mouth stimulation, we examined social gaze distance (defined as the average Euclidean distance between each fixation during the post-gaze epoch and the center of partner's Mouth) and non-social gaze distance (defined as the average Euclidean distance between each fixation and the center of the corresponding RDM stimulus). Wilcoxon signed rank test was used to compare social gaze distance between microstimulation and sham trial types. On the day level, none of the three brain regions had any microstimulation effect on social gaze distance (OFC: $p = 1$; dmPFC: $p = 1$; ACCg: $p = 0.125$; Wilcoxon signed rank, two-sided; when considering fixations in the ipsilateral hemifield and the contralateral hemifield separately, all $p > 0.18$) or non-social gaze distance (OFC: $p = 1$; dmPFC: $p = 0.188$; ACCg: $p = 0.188$; when considering fixations in the ipsilateral hemifield and the contralateral hemifield separately, all $p > 0.06$). Moreover, to control for unbalanced sample size between Eyes stimulation ($n = 27$ per area in total; $n = 15$ from monkey L and $n = 12$ from monkey T) and Mouth stimulation ($n = 5$ per area from monkey T), we first bootstrapped by randomly selecting 5 days with replacement from all the available data ($n = 27$) in Eyes stimulation for 1,000 times and compared the 1,000 medians to the true median in Mouth stimulation. For fixations in the contralateral hemifield, microstimulation effect (stimulation minus sham) of OFC led to significantly smaller social gaze distance in Eyes stimulation compared to Mouth stimulation ($p = 0.009$), while no effect was observed for fixations in the ipsilateral hemifield ($p = 0.724$) or when both hemifields combined ($p = 0.799$). To be more precise, we bootstrapped by randomly selecting 5 days with replacement from monkey T's data only ($n = 12$) in Eyes stimulation for 1,000 times and compared the 1,000 medians to the true median in Mouth stimulation and the differences were even more significant ($p = 0.005$ for contralateral; $p = 0.654$ for ipsilateral; $p = 0.510$ for both hemifields combined). While we did not test non-closed-loop microstimulation protocol, these findings suggested that even by applying closed-loop microstimulations in OFC with exactly the same parameters, stimulations effect could be modulated by the specific closed-loop protocol (i.e. what specific social gaze events triggered microstimulations; looking at Eyes vs. Mouth here).

Gaze latency analyses

To examine dynamic social attention in the temporal dimension, we examined two measurements, inter-looking interval and reciprocation latency. Specifically, we focused on the whole Face ROI and combined events when only M1 fixated on the whole Face of M2 and the events when both monkeys' gaze positions were within each other's whole Face. First, we examined inter-looking interval, the latency for M1 to look back at M2's whole Face within 5 sec after the onset of a microstimulation or sham (Figure 3A). Inter-looking interval was calculated for each trial and averaged across all microstimulation trials and sham trials separately for each day (Figure 3B; see Figure S3A for an alternative visualization). Wilcoxon signed rank test was used to compare such interval between microstimulation and sham trial types. Same analysis was applied for the non-social control condition by using the corresponding whole Face ROI. We also performed a trial-level analysis given that there was a relative low number of relevant gaze events by collapsing all microstimulation trials and all sham trials separately across all days for each stimulated brain region (Figure S3B). Wilcoxon rank sum test was used to compare inter-looking interval between microstimulation and sham trial types on the trial level.

We next examined reciprocation latency, the latency for M1 to look back at M2's whole Face after M2 looked at M1's whole Face within 5 sec after the onset of a microstimulation or sham (Figure 3C). Reciprocation latency was calculated for each trial and averaged across all microstimulation trials and sham trials separately for each day (Figures S3C and S3D). Wilcoxon signed rank test was used to compare such latency between microstimulation and sham trial types. Again, due to the scarcity of relevant gaze events, we collapsed all microstimulation trials and all sham trials separately across all days for each stimulated brain region (Figure 3D). Wilcoxon rank sum test was used to compare such latency between microstimulation and sham trial types. This analysis can only be applied in the live social gaze condition because there was no information about M2's gaze in the non-social control condition given that M2's visual access to M1 was blocked by the mini monitor placed in front of her.

Inter-individual gaze dynamics analyses

In addition to M1's gaze behaviors, we also examined how the two monkeys in a pair interacted with each other and their gaze directionality. By using moment-by-moment social gaze distance during the post-gaze epoch from each monkey (distance between one's gaze positions and the center of the other monkey's Eyes), we applied causal decomposition analysis[26] and calculated the average relative causal strength across all intrinsic mode functions (IMFs) for each trial. A relative causal strength value closer to 1 means stronger directionality from M1 (stimulated monkey) to M2 (partner monkey) and a value closer to 0 means stronger directionality from M2 to M1 (Figures 4A and 4B). Because the causal decomposition analysis required continuous data, we smoothed gaze data to fill in the gaps between fixations and excluded a trial if more than 1 sec continuous eye tracking samples of either monkey were 'NaN' or the start and end points of either monkey's smoothed portion were more than 20 visual degrees apart. Wilcoxon signed rank test was used to compare the relative causal strength between microstimulation and sham trial types (Figure S4A). Again, this analysis can only be applied in the live social gaze condition as there was no information about M2's gaze in the non-social control condition.

To further investigate microstimulation effect on a longer timescale, we divided microstimulations into early epoch (the first 45 stimulations) and late epoch (the next 45 stimulations) for each day. 76 out of 81 days had at least 90 stimulations. The 5 days excluded from further analysis were 1 day from monkey L with OFC microstimulations, 1 day from monkey T OFC, 2 days from monkey T dmPFC, and 1 day from monkey T ACCg. Wilcoxon signed rank test was used to compare the relative causal strength for different combinations of microstimulation trial types and time epochs (Figure S4B). Then, for each day, we fitted a linear regression between social gaze distance and relative gaze causal strength. This analysis was conducted by using social gaze distance in both hemifields combined, contralateral hemifield, and ipsilateral hemifield. Wilcoxon signed rank test was used to compare the slope of this fitted line between late epoch and early epoch separately for OFC, dmPFC, and ACCg (Figures 4C, S4C, and S4D). Lastly, to make sure the observed results were robust, we calculated the real median slope difference between late epoch and early epoch for each stimulated region and compared it to the null distribution of slope difference medians by shuffling the temporal order of the 90 microstimulations for 1,000 times for each day (Figures 4D, S4E, and S4F; permutation test).

Control analyses on current gaze events, pupil size, and saccades

To inspect if microstimulations resulted in any change in the current gaze event in the live social gaze condition, we first examined the average duration of current looking at partner's Eyes that triggered a microstimulation or sham (Figure 5A). These measurements were calculated for each day and Wilcoxon signed rank test was used to compare them between microstimulation and sham trial types for each stimulated brain region. We also compared the average pupil size aligned to the trial onset between microstimulation and sham trial types for each stimulated brain region (Figure 5B). Because pupil size is sensitive to eye movement as well as visual stimulus, for this analysis, we only selected trials in which the stimulated monkey's gaze position fell within the partner's whole Face throughout at least 700-msec following a microstimulation or sham. We averaged pupil size across trials within each day and for each 10-msec time bin, we compared pupil size between microstimulation and sham trial types for each stimulated region using Wilcoxon signed rank test. Then we examined the total number of microsaccades and macrosaccades during post-gaze epoch for microstimulation and sham trials. We identified saccades using an unsupervised clustering method[90] that captured both canonical microsaccades (small deviations in position within an epoch in which the eye is mostly steady) and macrosaccades (a more explicit saccade to a new spatial location). We thus separated microsaccades and macrosaccades in the following way: for each detected saccade event, if the event occurred strictly within an interval that was separately identified as a fixation,[89] we classified the event as a

microsaccade; otherwise, we classified the event as a macrosaccade. Wilcoxon signed rank test was used to compare the total number of microsaccades and macrosaccades between microstimulation and sham trial types for each stimulated brain region (Figures 5C and 5D). Lastly, we looked at M1's macrosaccades during the post-gaze epoch for each microstimulation or sham and calculated peak velocity (deg/sec) and amplitude (deg) for the first macrosaccade. Wilcoxon signed rank test was used to compare the average macrosaccade peak velocity between microstimulation and sham trial types for each stimulated brain region (Figure 5E). Moreover, for each day, we fit a linear regression between peak velocity and amplitude of all such first macrosaccades for microstimulation trials and sham trials separately and calculated the slope difference between the two trial types (Figure 5F). Wilcoxon signed rank test was used to compare such slope difference to zero. Within each day, we also created a shuffled null distribution of such slope differences by shuffling trial type label 1,000 times and compared the real median slope difference to the 1,000 medians of slope difference from the shuffled null distribution (Figure 5G; permutation test). Further, we categorized these macrosaccades into four groups depending on their direction ('II': saccades going from ipsilateral [I] hemifield to ipsilateral [I] hemifield; 'IC': saccades going from ipsilateral hemifield to contralateral [C] hemifield; also 'CI'; 'CC'). Wilcoxon signed rank test was used to test microstimulation effect on saccade kinematics against zero for each group separately (Figure 5H).